Kinetics of Solution Hardening

U. F. KOCKS

The flow stress of solution hardened single crystals and polycrystals is analyzed with respect to its dependence on temperature and strain rate. An evaluation of literature data, especially at low temperatures and low concentrations in fcc alloys, reveals that the interaction between dislocations and discrete, atomic-sized obstacles (or fixed clusters of them) cannot be responsible for solution hardening. A 'trough' model is favored in which the effect of the solutes is postulated to be equivalent to a continuous locking of the dislocations along their entire length, during every waiting period. The macroscopic features of this model are similar to Suzuki's chemical-hardening model. It can also explain the strong interaction of solution hardening and strain hardening at elevated temperatures, as well as basic features of dynamic strain-aging, in particular its strain dependence.

I. INTRODUCTION

THE effects of solutes on mechanical properties are manifold and virtually ever-present. They were one of the first to be considered in terms of dislocation theory[1,2] and are one of the last to be understood. There is an extensive and still active literature in the field, which may give the impression of a quantitative understanding including many details.[3] On the other hand, some basic issues are still seriously debated.

There are various kinds of interaction between solute atoms and dislocations. A useful classification of these interactions was discovered by Fleischer:[4,5] one large group is 'weak', another is 'strong'; the ratio of the interaction strengths is more than a factor of 10, with few if any materials in between. Strong interactions, giving rise to 'rapid hardening' (with concentration) are always due to solutes with tetragonal distortions, such as the defect pairs typically observed in ionic solids and presumably interstitials in bcc metals[4] (though see Leslie and Sober[6]). When such tetragonal distortions are not present, such as in substitutional solutions in metals, or interstitials in fcc metals, the various remaining solute/dislocation interactions are weak by comparison. We shall here be concerned only with the latter.

We will concentrate on the regime of behavior that has been perhaps the most widely studied: that near the so-called plateau stress at intermediate temperatures. Some of the materials to be considered exhibit abrupt yielding and/or jerky flow over some part of the regime, and others yield and flow smoothly throughout; they all show plateau-like behavior in an 'intermediate' temperature range. Our aim is to analyze a wide range of phenomena, relating to this central regime and contiguous regimes of behavior, and illustrate them by typical examples. This must unfortunately be at the expense of a general coverage of the literature, and of much important detail.

Solution hardening has classically been treated as a contribution to the 'friction stress', which shifts the whole stress/strain curve to higher stresses. The real situation is much more complicated; this will be reviewed in Section II. The interaction between solution hardening and work hardening is now widely recognized in its importance,[7–13] but a general theory is still elusive. We will merely outline the various phenomena. One consequence of this interaction is that even the yield stress is not in general free from any problems of superposition.

There is also a grain-size effect that depends on solute additions.[14–19] For this reason, the most reliable information on solute effects is from single crystals, or from polycrystals investigated over a wide range of grain sizes.

Section III surveys the temperature dependence of the yield stress and also, in some cases, of the ultimate tensile strength, for materials in which solution hardening and strain hardening are deemed to be the only operative mechanisms. A 'plateau' of flow stress over a significant temperature range can be identified, at least in some approximation, for a great variety of alloy systems. It is shown that the low temperature-sensitivity of the flow stress occurs at temperatures below the regime in which there is macroscopic evidence for solute mobility (which could be one reason for plateau-like behavior).[20–24]

This intermediate temperature regime is then analyzed in terms of two generic models of solution hardening: one in which the solute atoms act as *discrete* obstacles;[3,4,25] the other in which they provide '*troughs*' for the dislocation line energy (from which the dislocation must '*unlock*' repeatedly during its progress through the slip plane).[26,27] It is shown that there are order-of-magnitude arguments against the discrete-obstacle model, for the 'weak' obstacles considered here. The trough model, on the other hand, appears to describe basic features of the observations quite well.

Section IV summarizes how the instantaneous rate sensitivity of the flow stress can be used as a potent tool to identify the number and kind of operative mechanisms. This technique is applied to the particularly penetrating experiments of Basinski *et al.*[28] The analysis shows that, again, the discrete-obstacle model is untenable (at least for the tested alloys: fcc single crystals, substitutional solutions). This is so for four separate, solid reasons (including Basinski's 'stress equivalence'); and it is so even though these particular experiments relate to conditions in which the model would have been expected to apply if ever: very low concentrations and temperatures low enough to preclude any solute mobility by diffusive mechanisms.

Having shown that, on a strictly heuristic basis, a trough model has cardinal features that could explain the temperature dependence over a wide range, we explore in Section V some details of such models. It is also shown that

U. F. KOCKS is with the Center for Materials Science, Los Alamos National Laboratory, Los Alamos, NM 87545.

This paper is based on a presentation made at the symposium "50th Anniversary of the Introduction of Dislocations" held at the fall meeting of the TMS-AIME in Detroit, Michigan in October 1984 under the TMS-AIME Mechanical Metallurgy and Physical Metallurgy Committees.

a transition to the higher-temperature mechanisms can be made easily, by the simple expedient of limiting the length of the activated segment to the forest-dislocation spacing; this also provides a link to strain-hardening and strain-aging mechanisms.

In summary, we will show that a single sweeping assumption can rationalize all observations with ease: that the solutes behave as if they distributed themselves *continuously* along the dislocation lines, while these stop at 'hard-line' positions given by the forest structure. The physical mechanism responsible for this trough-digging effect is not clear, especially at low temperatures; some possibilities are explored. This basic assumption is, on a broader perspective, located between the two classical ones: that the solutes act as fixed discrete obstacles;[5] or that they behave as if they were smeared out in *two* (or three) dimensions.[1]

II. SOLUTION HARDENING AND STRAIN HARDENING

A. *Superposition of Mechanisms*

In practice, the flow stress is almost never controlled by a single mechanism. If one wishes to study a single mechanism, one has two options: attempt to find an 'academic' case where all other mechanisms are absent or investigate the superposition laws along with the other aspects of behavior.[29] Solution hardening is often coupled with a *lattice resistance*; we will avoid these cases by ignoring, *e.g.*, bcc metals at low temperatures.

Similarly, *grain-size* effects can be avoided by studying single crystals — but one must then assume, before applying the results to a polycrystal, that the behavior of a representative grain is the same as that of a free single crystal. Most generally, one must study polycrystals at various grain sizes, ascertain the superposition law, and extrapolate to infinite grain size. The common alternative to investigate properties at a *constant* grain size, however, would have to assume that the grain-size contribution to the flow stress is either negligible or independent of concentration, which has often been demonstrated to be untrue.[14–19]

One contribution to the flow stress that can never be avoided is that due to strain hardening. Even the *yield stress* generally involves dislocation/dislocation interactions, as is evident from the finite yield stress of the purest single crystals (even in the absence of a lattice friction). This contribution increases with strain; thus a comparison of entire stress/strain curves, not just of yield stresses, for different alloys should shed light on the superposition between solute/dislocation interactions and dislocation/dislocation interactions. In the following sections, we will survey the types of behavior observed.

B. *Additivity*

The most common assumption is that solute atoms provide a *friction stress* τ_f, which adds to all other contributions;[25,30,31] in particular:

$$\tau = \tau_f(c) + \tau_d(\rho) \qquad [1]$$

where τ_d is due to dislocation/dislocation interactions: it depends on the dislocation density ρ; the friction stress depends on the solute concentration c. The total glide resistance is called τ; this symbol is used instead of σ in order to emphasize (a) that it is a material property (and a scalar), not an applied stress (a tensor); and (b) that it describes the resistance to crystallographic shear, to be converted into a macroscopic stress value by use of an appropriate (average) orientation factor (which may itself depend on strain).[32]

If Eq. [1] were strictly true, solute additions should lead to an upward shift of the entire stress/strain curve. This is rarely observed.[7,12] Figure 1 shows one of the few examples[33] — albeit for a rather small range of strains. Some other alloys for which such behavior has been observed are Cu-Au,[34] Cu-Ni,[34] and Th-C,[35] all polycrystals and all at relatively small strains and low temperatures. In these cases, the contribution from solution hardening is easily identified; in particular, its definition as

$$\Delta\tau = \tau_Y - \tau_Y(\text{pure}) \qquad [2]$$

is appropriate (so long as there is no solute dependent grain-size effect). This is by no means generally true.

C. *Multiplicative Hardening*

An empirical observation that is at least as common as additivity is a *proportionality* between solute hardening and strain hardening: the stress/strain curves diverge with increasing strain.[12,13,36] Allowing also for an additive friction stress, this can be written as

$$\tau = \tau_f(c) + [1 + k(c)] \cdot \tau_d(\rho) \qquad [3]$$

The term $k \cdot \tau_d$ amounts to an *interaction* between solution hardening and strain hardening. It would exist also at the yield stress; thus, Eq. [2] does not hold under these conditions.

Classical examples of this behavior are Al-Mg[37] and Cu-Al,[38] and a recently investigated one is Ni-Mo[36] (Figure 2). It is clear that the polycrystal stress/strain curves diverge. While these alloys all exhibit dynamic strain-aging to a greater or lesser extent, the multiplicative effect on hardening is present outside the temperature regime of jerky flow.

D. *Other Superposition Laws*

Additivity (Eq. [1]) has been justified theoretically on the basis of treating both solutes and forest dislocations as discrete obstacles, but of vastly different densities and strengths.[30] More sophisticated statistical treatments[39,40,41] claim that

$$\tau^n = \tau_f^n + \tau_d^n \qquad [4]$$

with $n > 1$, should be a better approximation. Certainly, for obstacles of equal strengths, one should expect Eq. [4] with $n = 2$, since their densities should add (and the flow stress is assumed to be proportional to the square root of the area density of obstacles).

The effect of a superposition law of the form [4] (with $n > 1$) on the linearly plotted stress/strain curves is to make those of the alloys concave upward (when that of the pure materials is straight).[29] Such behavior is typically observed for irradiated materials (where, according to the above, it should be expected); I am not aware of any case in which such concavity has been observed in polycrystalline dilute solid solutions.

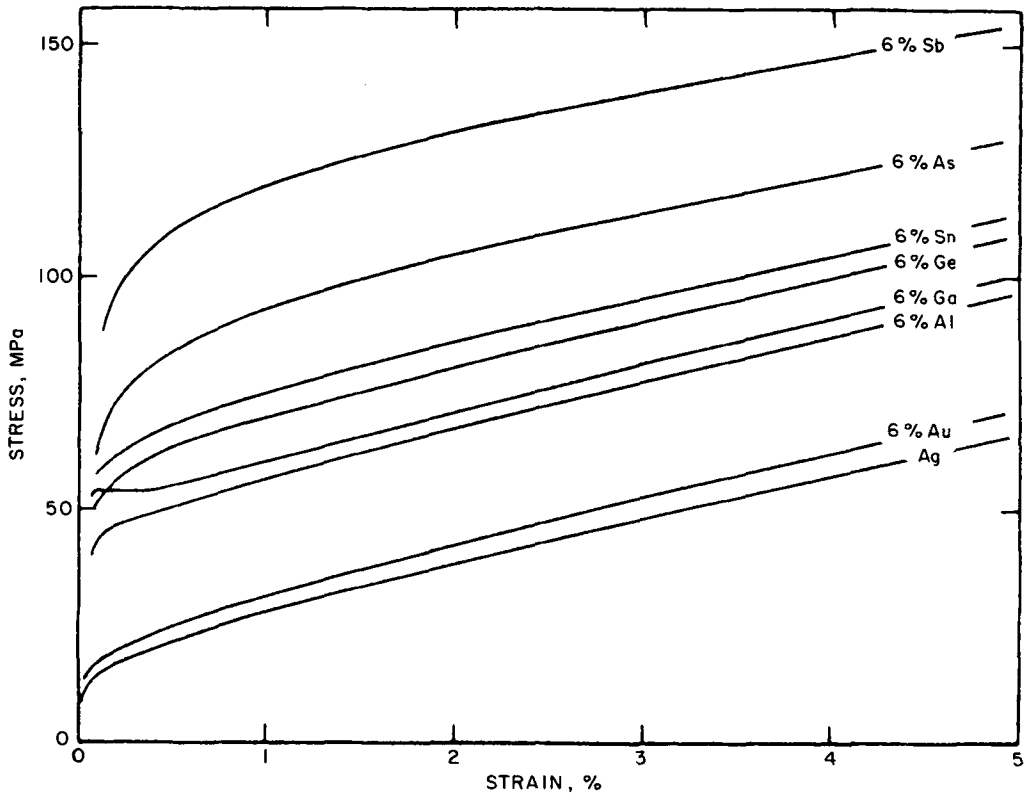

Fig. 1 — An example of additivity between solution hardening and strain hardening: stress strain curves for various polycrystalline silver alloys at 77 K, all at 6 at. pct concentration. Note the small strain range. After Hutchison and Honeycombe.[33]

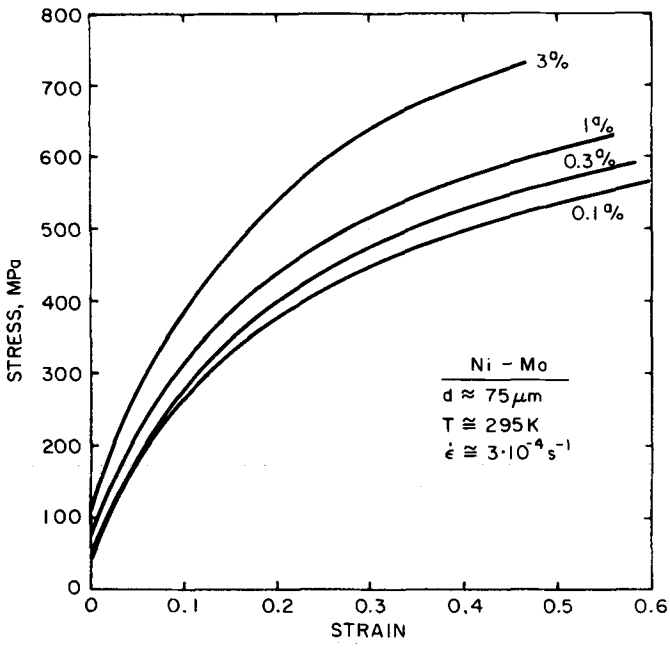

Fig. 2 — An example of multiplicative solution hardening: stress strain curves of four polycrystalline Ni-Mo alloys at room temperature, to large strains. After Bloom, Kocks, and Nash.[36]

E. *Abrupt Yielding*

In many cases, especially at low temperatures, solution hardened alloys show an abrupt yield drop and the concomitant propagation of a Lüders band along the length of the specimen. This is associated with some difficulty to *generate* mobile dislocations (from stabilized 'atmospheres' or segregations). Note, however, that at the *end* of this Lüders extension, the whole sample has suffered the macroscopic strain; at this point, solution hardening contributes only a *propagation* stress, which superposes with strain hardening.[42] If the superposition is linear (Eq. [1]), a back-extrapolation to the elastic loading line gives the solution hardening contribution; if it is not, the *lower yield point* is the most appropriate measure, neglecting strain hardening.

Note that a similarity of behavior at the lower yield point and farther along the stress/strain curve is expected, since both relate to the propagation stress; only the upper yield point is caused by a generation stress. (It is also strongly influenced by stress concentrations and machine effects, and is therefore not usually of interest from a materials-characterization point of view.)

F. *Single Crystals*

Single crystals oriented for single slip show an initial region of 'easy glide'. This tends to complicate interpretations a bit (and is irrelevant for applications to polycrystal deformation). Figure 3(a) shows an example:[43] while the yield stress increases monotonically with concentration, the rest of the stress/strain curve does not. This is because the *length* of easy glide initially increases with concentration, and its slope decreases.[44,45] The stress at the beginning of 'stage II' strain-hardening (the steep part) again increases with concentration, and it may be the most relevant for the yield stress in polycrystals.[46]

Despite these complications, single-crystal results reported in the literature are usually given in terms of the yield stress at the beginning of easy glide (the critical resolved shear stress: CRSS)—and, in fact, often merely as the excess over the value for the pure material (Eq. [1]). This may be misleading in considerations of the concentration dependence, for the following reason. A typical CRSS of a 'pure' single crystal is $10^{-5}\ \mu$ (where μ is the shear modulus). Such a value could itself be due to trace impurities: it would require only about 50 at. ppm of a typical substitutional solute. A back-extrapolation of the linear relation between the CRSS and the square root of the dislocation density in 'pure' materials does in fact suggest a small contribution from impurities.[47]

Figure 3(b) (from the same alloy at a different temperature) shows two additional features. First, the initial part exhibits a *zero* slope, associated with the spreading of a Lüders band along the single crystal. Then, the stress at the *end* of the nonuniform deformation should be the most relevant.

Second, Figure 3(b) shows an influence of solute concentration on the beginning of 'stage III' deformation: a delay in the onset of dynamic recovery. This has been rationalized in terms of a decrease in the stacking-fault energy with concentration in many alloy systems[25,48]—especially since it was also observed in Ni-Co alloys,[49,50,51] in which the change in SFE is assumed to be the major effect of solute addition.

G. *Dynamic Recovery*

The influence of solutes on dynamic recovery is, in fact, a wide-spread effect.[12,52] Interestingly, it also occurs in the interstitial Ni-C alloy (Figure 4).[53] Here, one would not assume a change in the stacking-fault energy. We conclude that solutes, in general, impede the rearrangement of previously stored dislocations, by whatever mechanism. Certainly, the width of extended dislocations (and thus the SFE) plays a significant role in this—but apparently not the only one.

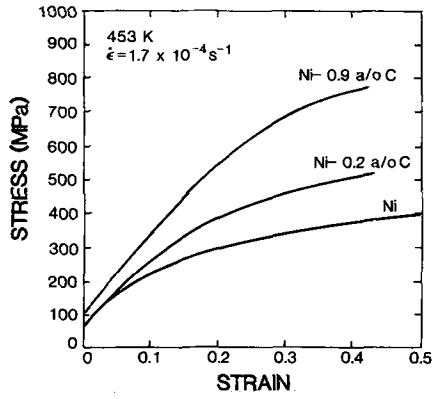

Fig. 4—Low carbon additions to nickel polycrystals cause an increase in yield, a multiplicative hardening, and a strong effect on dynamic recovery, which is presumably *not* due to a solute dependence of the stacking-fault energy. After Kocks, Cook, and Mulford.[53]

H. *Very Large Strains*

Finally, there appears to be a significant influence of solutes on the stress/strain curve at strains in excess of 1. Figure 5 shows a well-known example.[10] Such an effect could be merely a consequence of the previous one: the flow stress at large strains is primarily determined by a balance between strain hardening and dynamic recovery. However, even the nature of the stress/strain behavior seems to be affected: in the presence of solutes, a new linear stage of strain-hardening sets in at large strains, of low but definitely finite slope, whereas pure materials usually tend toward saturation.[54,55]

I. *Conclusion*

More often than not, there is a significant interaction between solution hardening and strain hardening. For this reason, the difference between the yield stresses of alloys and the pure material is not a good general measure of solution hardening, and a theory relating to yield stresses

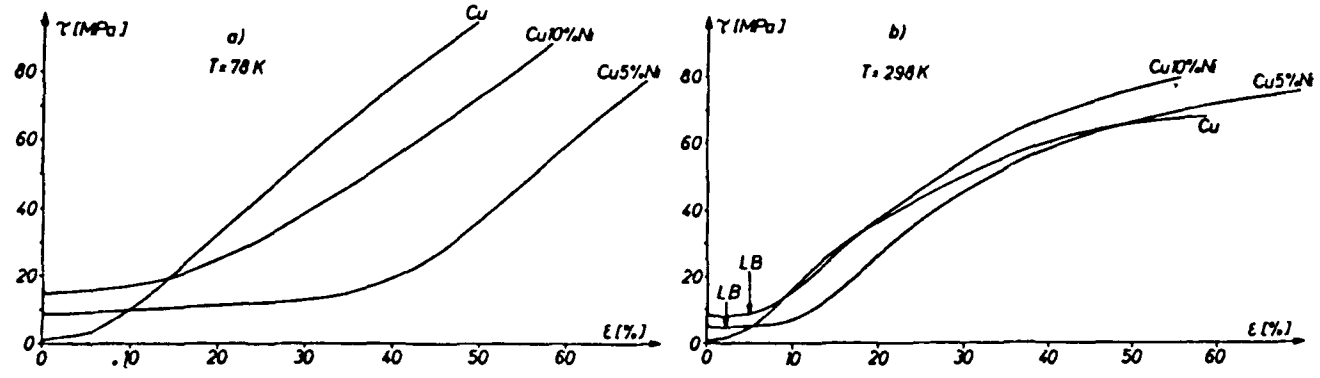

Fig. 3—Effect of nickel additions to copper single crystals: the yield stress increases monotonically, but the rest of the stress strain curve does not. After Neuhäuser *et al.*[43]

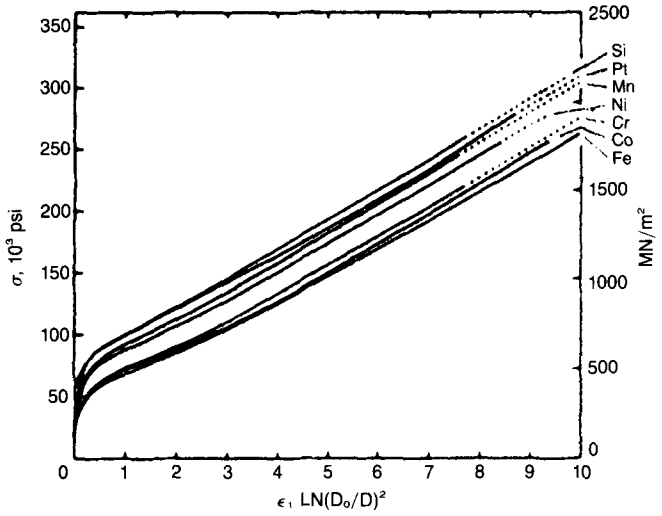

Fig. 5—Effect of solute addition to Fe at very large strains. All alloys contain 3 at. pct solute and were tested in tension after wire drawing, at room temperature. After Leslie.[10]

only is not likely to be general in describing the principal effects.

III. THE TEMPERATURE DEPENDENCE OF THE FLOW STRESS

A. *Survey of Observations*

Figures 6(a) through 6(d) show one example for each of the following cases of solution hardening: fcc, cph, and bcc substitutional alloys, and an fcc interstitial alloy.[33,56–58] Two of them relate to single crystals, and the rest to polycrystals. The different curves within each figure correspond to different concentrations of the same solute, except in Figure 6(a), which displays seven different solutes, all of the same atomic concentration.

The most evident feature of these figures is that they are all so similar: in every case, there is a relatively steep drop at low temperatures, followed by a 'plateau' (or something similar) at higher temperatures. *Both* regimes are concentration dependent, and the transition between them occurs at about room temperature or a little above. This similarity persists despite the fact that some of the 'yield stresses' correspond to a 'lower yield point' and thus to Lüders front propagation, others to smooth yielding; and that some of the alloys exhibit jerky flow at higher temperatures and some do not.

In some cases, the similarity may perhaps be fortuitous. In bcc metals, some solution *softening* is frequently observed at low temperatures. In cph crystals, it is generally assumed that the temperature dependence of slip is controlled by the lattice resistance—but perhaps not of basal slip, which was chosen for Figure 6(d). However this may be, it would seem unlikely that entirely different mechanisms explain the behavior of each different type of material.

The alloys illustrated in Figure 6 were, as stated, just examples; others show very similar behavior. Among fcc substitutional alloys, there are silver alloys,[28,33,59–63] gold alloys,[64] aluminum alloys,[65,66] nickel alloys,[49–51,67] lead alloys,[68] and a large number of copper alloys.[14,27,38,48,69–79] Another interstitial fcc alloy, in addition to the Ni-C,[56] is Th-C.[35] Basal slip in substitutional cph alloys has been investigated additionally in Mg-alloys[80–83] and in Zn-Cd.[84,85] Among bcc substitutional alloys, Ta alloys[86,87] exhibit similar behavior to the Nb-alloys,[57,88] and iron-alloys[10,89–92] at least show similar high-temperature behavior.

B. *Dynamic Strain-Aging*

A recurring suggestion has been that the 'plateau' in the flow-stress *vs* temperature relation is due to solute *mobility*.[20–24] Certainly, solutes do become mobile above

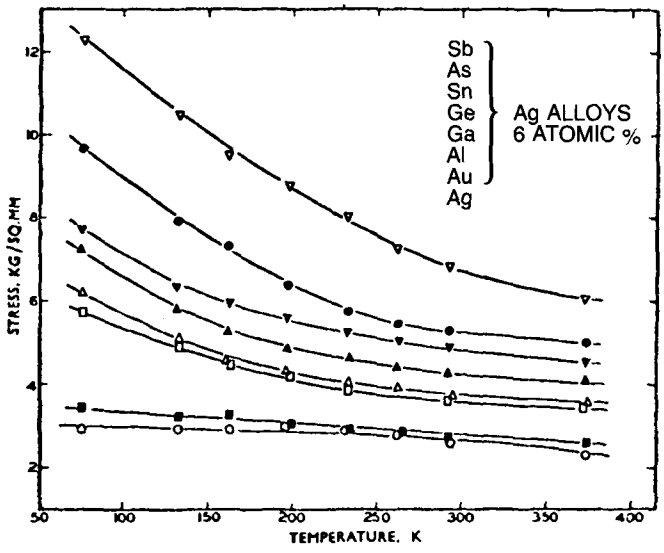

(*a*)

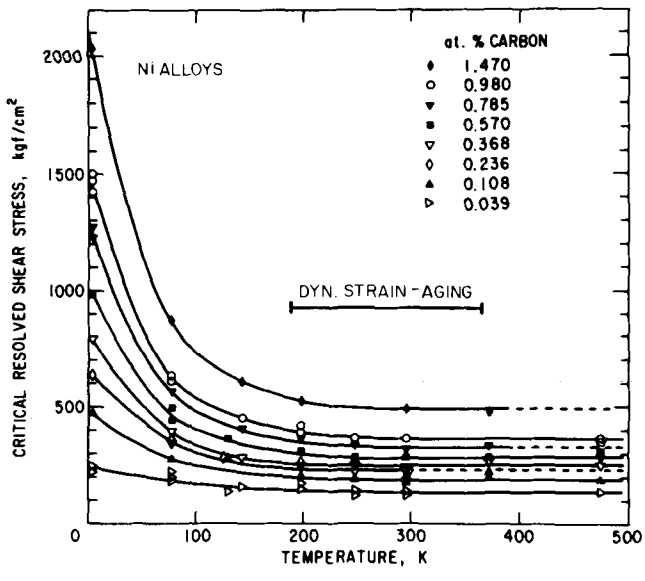

(*b*)

Fig. 6—Flow stress *vs* temperature for various alloy systems: (*a*) silver alloy polycrystals (fcc substitutional);[33] (*b*) Ni-C polycrystals[56] (fcc interstitial); (*c*) Nb-Mo single crystals[57] (bcc substitutional); and (*d*) Mg-Li single crystals[58] (cph substitutional). Some show sharp yield drops, some jerky flow, some neither—all show 'plateau'-like behavior.

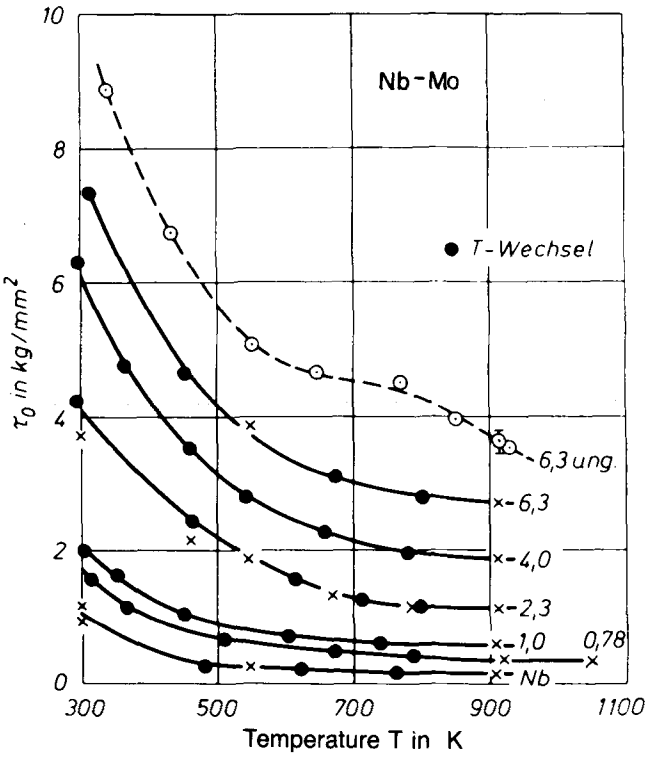

(c)

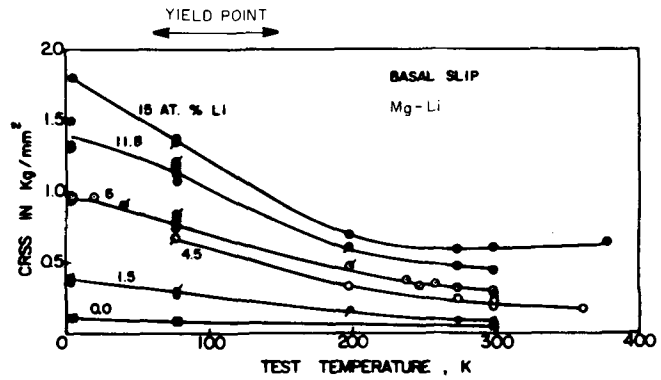

(d)

Fig. 6—Flow stress *vs* temperature for various alloy systems: (*a*) silver alloy polycrystals (fcc substitutional);[33] (*b*) Ni-C polycrystals[56] (fcc interstitial); (*c*) Nb-Mo single crystals[57] (bcc substitutional); and (*d*) Mg-Li single crystals[58] (cph substitutional). Some show sharp yield drops, some jerky flow, some neither—all show 'plateau'-like behavior.

some temperature and will then tend to segregate to dislocations (or away from them if the interaction should be repulsive, as is possible in the case of screws). This increases the flow stress, in the temperature range where the solute mobility is sufficient.

Figure 7(b) shows the hump in the flow stress *vs* temperature diagram that should follow from such a mechanism;[66] Figure 7(a) shows an equivalent—but more microscopic—measure of the breaking strength from internal-friction

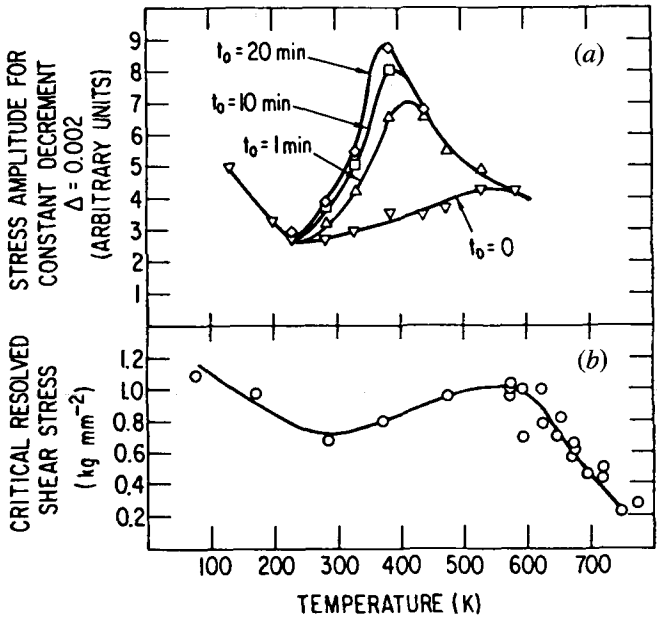

Fig. 7—Dynamic strain-aging is evidenced by the time- and temperature dependence of an internal-friction measure of the obstacle strength (*a*), and (*b*) by a hump in the flow stress *vs* temperature diagram, for Al-1 at. pct Mg. After Schwarz.[23]

measurements.[23] Its time dependence means that the phenomenon must be due to solute mobility.

In most materials, however, the flow stress decreases monotonically with temperature. One trivial reason for this is that the shear modulus decreases with temperature and contributes to a negative slope; thus, a *zero* slope in τ *vs* T would already be positive in τ/μ *vs* T. Furthermore, there could be a sufficiently negative slope left from the low-temperature mechanism (whatever it is) to offset a slight positive contribution from dynamic strain aging. Of course, one would not expect an exactly flat 'plateau' from such a superposition—but the observed 'plateaus' are rarely long enough to allow a real assessment of their flatness.

A hump is frequently observed in a diagram of *ultimate tensile strength* (or saturation stress) *vs* temperature (Figure 8).[93,94,95] Firstly, this demonstrates that strain hardening is greater in this temperature regime: an observation generally made in connection with dynamic strain-aging. Secondly, if solute mobility is obvious at large strains, it is likely to be present at low strains, too.

An even more obvious indication of solute mobility is the occurrence of jerky flow (the Portevin-LeChatelier effect): it is a consequence of an inverted strain-rate (rather than temperature) sensitivity.[42,96] In some cases, the observation of jerky flow has been explicitly noted in connection with solution-hardening experiments. Figure 9 demonstrates such a case.[75] Here, the occurrence of jerky flow exactly coincides with the plateau-like behavior (even though a 'hump' is not observed until the *end* of this temperature range). Other cases like this are Cu-Zn[75] and Cu-Al.[97]

Inverted temperature and rate sensitivities, and jerky flow, are only extreme exhibitions of solute mobility. In the next chapter, we shall see that more subtle tests demonstrate the existence of solute mobility over a much wider range of conditions, and in more cases.

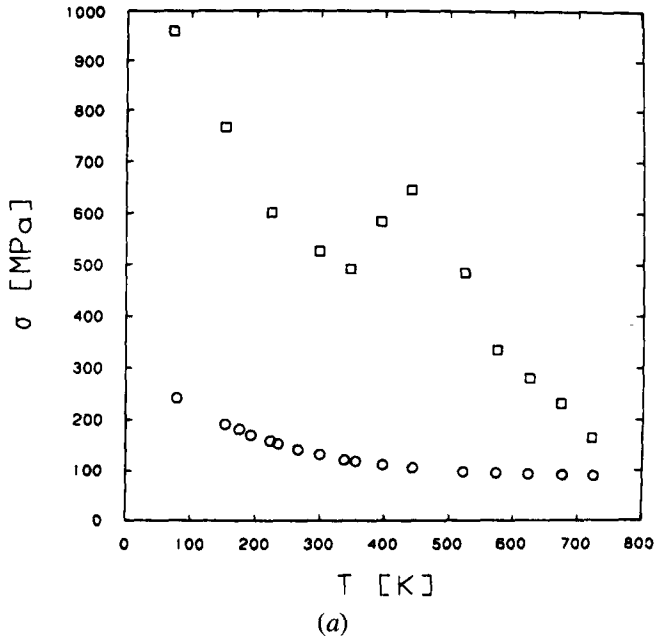

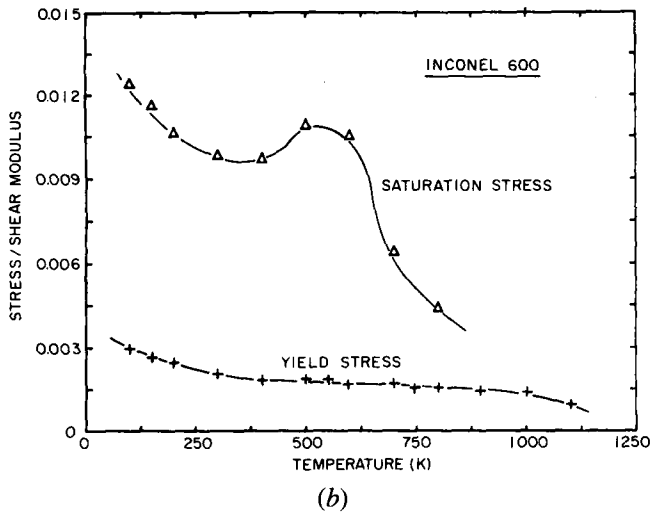

Fig. 8—Temperature dependence of (*a*) yield stress and ultimate tensile strength for Cu-Sn polycrystals,[93] (*b*) yield stress and saturation stress for INCONEL 600.[94] The 'hump' in the curve due to dynamic strain-aging is usually only evident at large strains.

In summary, plateau-like behavior is certainly sometimes, and possibly always, correlated with solute mobility. However, we shall demonstrate in the next section that plateau-like behavior begins in many cases at lower temperatures than any evidence (or plausibility) of solute mobility; this is a major problem for modeling attempts.

C. *The Discrete-Obstacle Model*

The model that has dominated interpretations of solution hardening over the last 20 years[3,25,98] was first proposed, as one contribution to solution strengthening, by Friedel,[2] and was then elaborated in detail by Fleischer.[4] As distinct from

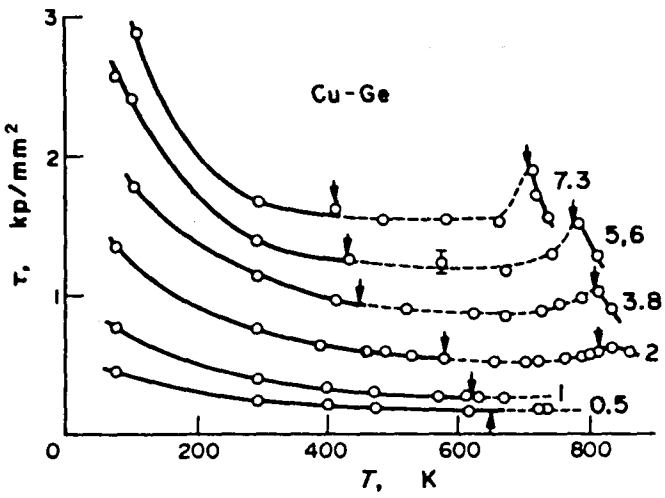

Fig. 9—CRSS *vs* temperature for Cu-Ge single crystals of various atomic concentrations. The regime of jerky flow is shown dashed; plateau-like behavior is evident even at lower temperatures. After Traub *et al.*[75]

the previous models of Mott and Nabarro,[1] in which solutes were considered essentially as if they were smeared out in two or three dimensions (and acted on dislocations only through fluctuations in this distribution), it is assumed here that solutes act like discrete particles, being overcome by the dislocations individually. This makes a treatment by thermal-activation theory straightforward. It is precisely these straightforward considerations that offer a serious contradiction to the model.[98] This contradiction has, in our opinion, not been taken seriously enough until now.

Figure 10 shows a typical dependence of the activation energy ΔG on the stress τ_f, for a single set of discrete

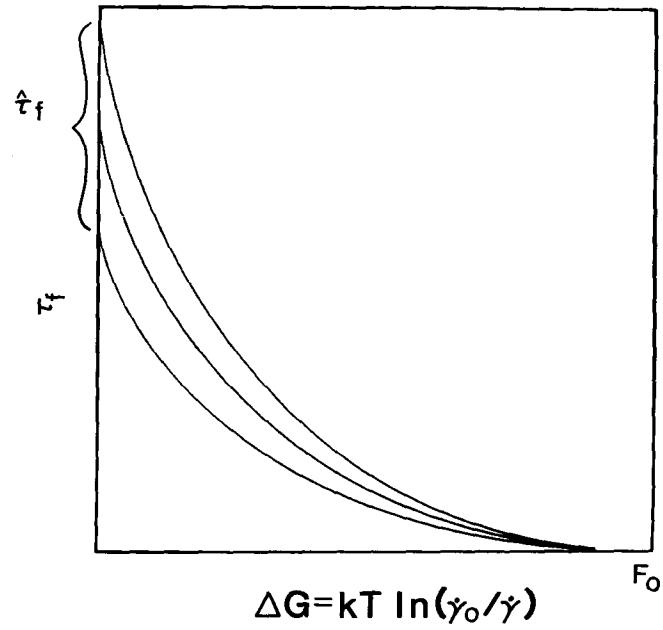

Fig. 10—Schematic of temperature dependence of friction stress τ_f (at constant strain rate $\dot{\gamma}$) for various concentrations of the same alloy according to the discrete-obstacle model. The total interaction energy F_0 limits the temperature up to which an effect should be observable.

obstacles. (We write τ_f to avoid the problem of superposition; see Section II.) The activation energy is plotted on the abscissa because it is, according to the Arrhenius equation, proportional to temperature (at a given strain rate $\dot{\gamma}$):

$$\Delta G = kT \ln(\dot{\gamma}_0/\dot{\gamma}) \quad [5]$$

where k is Boltzmann's constant and $\dot{\gamma}_0$ a pre-exponential factor.*

*It has been demonstrated that the assumption of a *constant* $\dot{\gamma}_0$ is appropriate whenever the rate sensitivity is low; the stress dependence of the mobile dislocation density is then negligible with respect to that of the dislocation velocity — which is then, in turn, essentially equivalent to that of the strain rate.[30] Also note that back jumps are neglected.

Figure 10 shows two limits: a stress $\hat{\tau}_f$ at which no thermal activation is needed (in the limit of zero temperature), and a total activation energy F_0 (in the limit of zero stress). Near both limits, the curve must be parallel to the respective coordinate axis, for all realistic interaction laws and obstacle arrangements.[30]

The total interaction energy F_0 between one solute atom and a dislocation determines the highest temperature, T_0, at which this interaction can contribute to the flow stress. We wish to find an upper limit for this temperature. From Eq. [5], and using the observation that the logarithmic factor is at least 16 (typically 20), for most common strain rates and mechanisms, we have

$$kT_0 \leq F_0/16 \quad [6]$$

On the basis of physical mechanisms, one might expect F_0 to be a few tenths of an electron volt. It is, however, possible to come up with a quantitative estimate on the basis of the model itself and some macroscopic observations. The argument goes as follows.

The interaction can be specified in terms of a force-distance diagram. Its major characteristics are a maximum force, $\hat{K}$, and an average width, $\overline{\Delta y}$. Then the total interaction free-energy is

$$F_0 = \hat{K}\,\overline{\Delta y} \quad [7]$$

The average width cannot be more than a very few atomic spacings (keeping in mind that it relates only to the resisting part of the interaction profile, on *one* side of the solute). Say, it is $\leq 3b$, where b is the magnitude of the Burgers vector.

The maximum interaction force can be derived from the maximum flow stress, $\hat{\tau}_f$. With the statistics appropriate for low concentrations of weakly binding solutes,[2,30] the relation is

$$\hat{\tau}_f = \left(\frac{\hat{K}}{\mu b^2}\right)^{3/2} \mu\sqrt{c} \quad [8]$$

where μ is an appropriate shear modulus and c the atomic concentration. The quantity $\hat{K}/\mu b^2$ is the interaction strength normalized by twice the dislocation line tension; it determines the angle by which a single solute atom can bend the dislocation.[30]

As Fleischer pointed out,[4,5] solute atoms fall in two classes: 'weak binders' (all substitutional solutes in metals, plus interstitials in fcc metals, and others), for which $\hat{K}/\mu b^2$ comes out to be between about 1/60 and 1/80, from an analysis of measured values of $\hat{\tau}/\mu\sqrt{c}$; and strong binders (interstitials in bcc metals, for example), for which it is $>1/10$. Thus we find, *for weak solutes*,

$$F_0 = \mu b^3 \frac{\hat{K}}{\mu b^2}\frac{\overline{\Delta y}}{b} \leq \frac{1}{20}\mu b^3 \quad [9]$$

For copper alloys, this gives a limit $F_0 \leq 0.2$ eV, which is typical and plausible. For the critical temperature, we get the upper limit

$$kT_0 \leq \mu b^3/320 \quad [10]$$

which is 1/80 eV for copper, or $T_0 \leq 150$ K.

Yet we find that the end of the steeply declining part of the flow-stress temperature diagram is not reached until at least double that temperature for copper alloys. Obviously, there is no possibility at all for discrete-obstacle interactions to be responsible for the plateau itself: they are too easy to activate thermally. The surprise is that they do not seem to be able to account even for the low-temperature behavior (assuming some unexplained additional stress accounts for the plateau). To reiterate the point: all parts of the above estimate were made in the *limit* that would be most favorable to the model; the actual discrepancy is likely to be *more* than a factor of 2 in temperature scale.

D. *The Temperature Dependence of the Shear Modulus*

So far, we have glossed over an important effect on the flow-stress *vs* temperature diagram, and that is the temperature dependence of the shear modulus. In virtually all models, the flow stress comes out proportional to the modulus (and if not, then to some other property of the interatomic potential at a given temperature, which may well depend on temperature as does the modulus). The normalization of the flow stress with the temperature-dependent shear modulus is taken care of by many authors. Another normalization is, however, rarely accounted for, and it is just as important for a quantitative analysis of the models. This is the normalization of the temperature with μb^3. It follows from a very simple argument:[30] the activation area, $-(\partial \Delta G/b\,\partial\tau)_T$, cannot be proportional to the modulus, since it is a geometric quantity. For this reason, ΔG must be proportional to μ whenever τ is (and b^3 appears for other reasons[30]). Thus, the general combination of variables for thermally activated flow is

$$\frac{kT}{\mu b^3} \cdot \ln\frac{\dot{\gamma}_0}{\dot{\gamma}} = \frac{\Delta G}{\mu b^3} = g\left(\frac{\tau}{\mu}\right) \quad [11]$$

The function g describes the dependence of the normalized activation energy $\Delta G/\mu b^3$ on the normalized stress τ/μ, where μ is to be inserted as $\mu(T)$ for *both* variables; the limiting values must be $g \to 0$ for $\tau \to \hat{\tau}$ and, for short-range obstacles, $g \to F_0/\mu b^3$ for $\tau \to 0$.

E. *The Trough Model*

In Section III-C, we have discussed the discrete-obstacle model from the point of view of its self-consistency and its fit with some qualitative experimental data, but without judging its physical basis. In this section, we shall do the same for the 'trough model'. It was invented[99] to describe the *unlocking* of dislocations from segregated solute atmospheres (in particular, in Fe-C), and has been used in descriptions of internal friction.[100,101] We will assume that it

might potentially describe *repeated* unlocking, too (*i.e.*, a propagation stress[26,27]), and discuss the physical basis for this later.

The most eye-catching property of trough models is that the activation energy is proportional to the *reciprocal* of the stress; this leads to a high-temperature branch of the τ *vs* T diagram in which $\tau \propto 1/T$: a very slow decay — almost plateau-like! Figure 11 shows Fisher's original fit, along with a simplified sketch of his model. While the solutes are shown individually, they are treated as if they were smeared out along the dislocation, giving it a lower line energy: one may say that the solutes make a *trough* for the dislocation. To move on, the dislocation has to leave the bound state and re-acquire its higher, 'free' line energy. It does so by nucleating a *bulge*; its curvature is given by the applied stress, the angle Y by the equilibrium between the two line tensions. The 'long-range' nature of the model comes from the fact that the dislocation has *everywhere* a high line energy, compared with the bound state.

At low temperatures, the original, simple model does not describe the behavior even of Fe-C. This is due to the assumption of just two discrete line energies; in other words, of a *square-well* potential for the interaction of the dislocation with a smeared-out string of solutes. Any realistic potential will have finite slopes; the maximum slope is the flow stress at zero temperature. The simplest potential that has this property is the *triangular well*; it gives for the activation energy of bulge nucleation[30]

$$\Delta G = \frac{4}{3}\sqrt{2\mathcal{F}_D\mathcal{F}_B}\,w \cdot \frac{\mathcal{F}_B}{\tau bw} \cdot \left(1 - \frac{\tau bw}{\mathcal{F}_B}\right)^{1/2} \qquad [12]$$

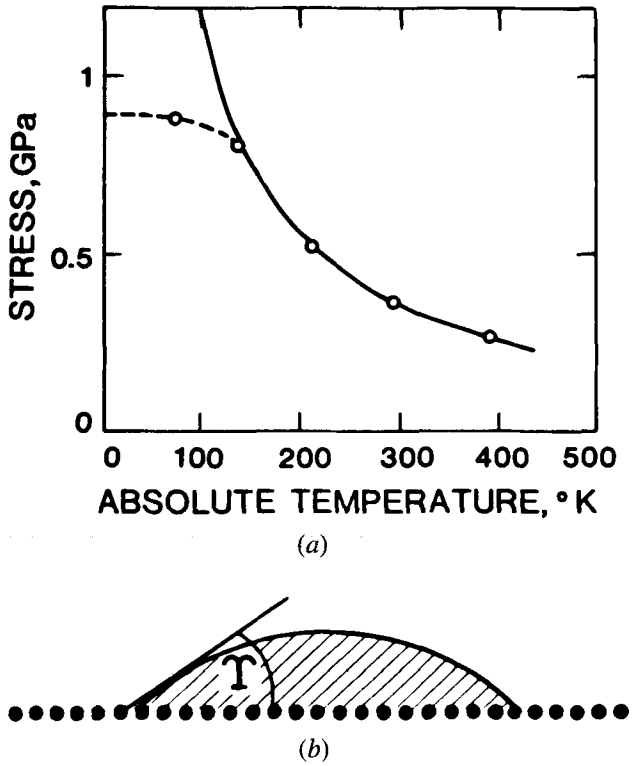

Fig. 11 — Thermally activated nucleation of a 'bulge' from a 'trough': (*a*) schematic. (*b*) At 'high' temperatures, it gives a reciprocal relation between flow stress and temperature.[99]

where $\mathcal{F}_D$ is the free energy per unit length of the free dislocation, $\mathcal{F}_B$ the binding free energy per unit length, and w the effective width of the trough (here, the half-width of the energy well; a more general definition of w will be given in Section V-D). For further use, we will introduce the following normalizations:

$$f_B \equiv \frac{\mathcal{F}_B}{\mu bw} \qquad [13a]$$

$$S \equiv \frac{\tau}{\mu f_B} \qquad [13b]$$

$$\psi \equiv \frac{4}{3}\left(\frac{2\mathcal{F}_D}{\mu b^2}\right)^{1/2}\left(\frac{w}{b}\right)^{3/2} \qquad [13c]$$

The constant ψ is supposed to contain whatever combination of effective dislocation line tensions is appropriate, instead of $\mathcal{F}_D$ itself, when anisotropy is properly accounted for.[30] One would expect it to be a little larger than 1.

Now, with Eqs. [5] and [12],

$$\frac{kT}{\mu b^3}\ln(\dot\gamma_0/\dot\gamma) = \frac{\Delta G}{\mu b^3} = \psi\sqrt{f_B}\cdot\frac{g(S)}{S} \qquad [14]$$

where $g(S) = \sqrt{(1 - S)}$ in Eq. [12], but may be a more general function in later applications: it plays the role of the *short-range* effect of the interaction profile; $g(S)$ must go to zero for $T \to 0$, and to 1 for $S \to 0$.

Short-range interactions are difficult to derive in detail and should depend on the solute. Suzuki, in fact, derived the square-root function (Eq. [14]) on the basis of a specific, detailed model (stacking-fault locking). We shall show in Section V that a *linear* relation should generally hold in the limit of low stresses in any trough model.

The salient feature of Eq. [14] that is independent of the local interaction is the dependence on the reciprocal of the stress. This suggests that a plot of *temperature-times-stress vs* stress is opportune: it should go to a *finite* value in the limit $S \to 0$. Thus, it has replaced the 'tail' in a τ-T plot by a (linear) decrease.*

*On the other hand, if the real behavior is *not* described by $\tau \propto 1/T$, but, *e.g.*, by a discrete-obstacle model, then the τ-*vs*-τT plot should curve back toward the origin as $\tau \to 0$.[30]

A second feature of Eq. [14] is most important: while the stress is normalized by the interaction strength f_B (Eq. [13b]) as expected, the temperature normalization *also* depends on f_B (its square-root); thus *both* scales are concentration dependent. This is due to an obvious property of the model: that the lowering of the line tension (and thus the total activation energy) is proportional to the linear density of solutes along the dislocation. As a consequence, the concentration dependence of the flow stress at a fixed (not normalized) temperature is meaningless. (Furthermore, as emphasized before, *both* stress and temperature are normalized by $\mu(T)$.)

In Figures 12(a) through 12(d), we have plotted diverse data on copper alloys according to this scheme: first, the stress and temperature were both normalized with $\mu(T)$;+

+The temperature dependence of b was ignored.

then, a value of $\ln(\dot\gamma_0/\dot\gamma)/\psi$ for each solute (ψ could depend on the interaction range w and on the elastic anisotropy),

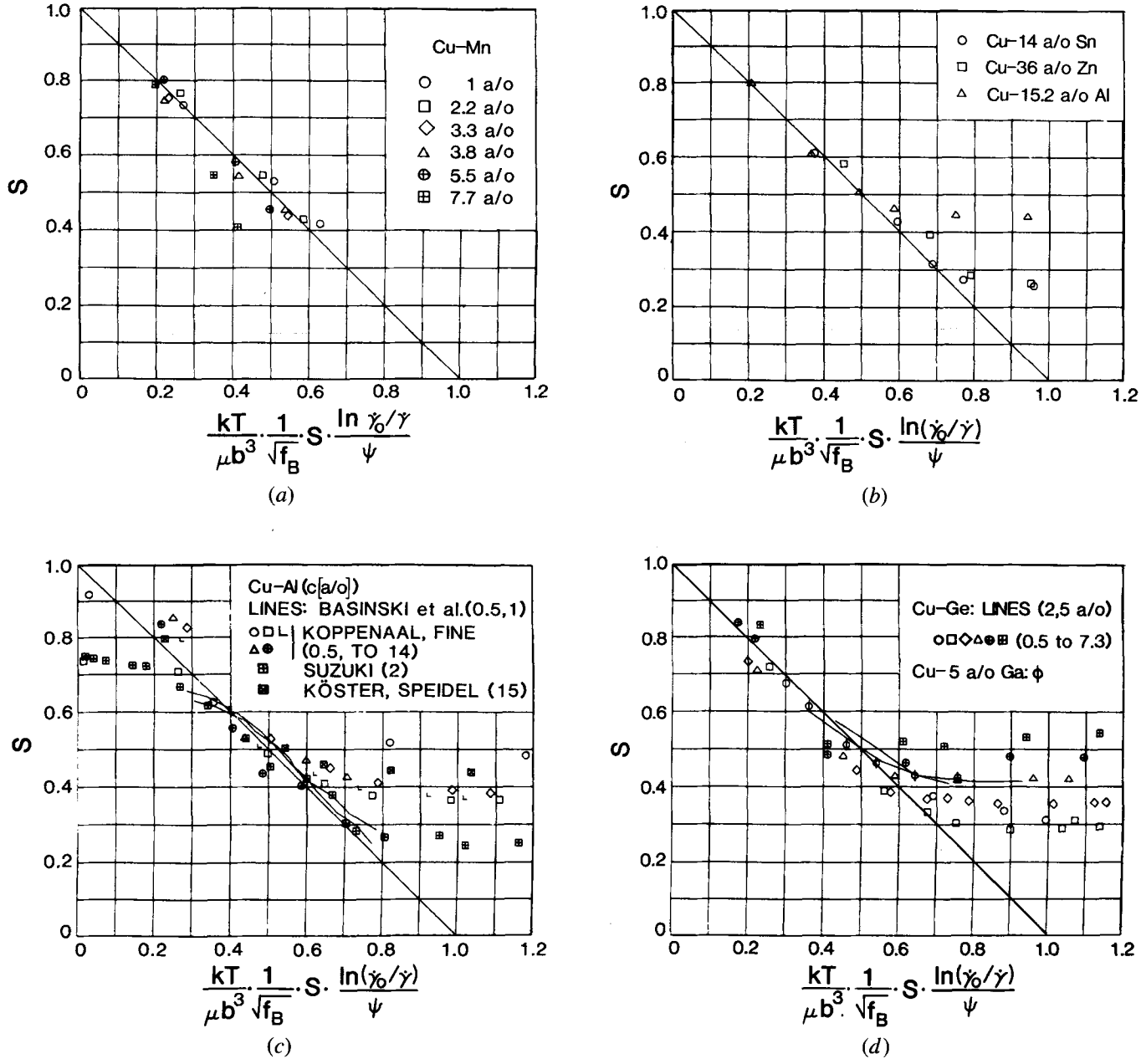

Fig. 12—Normalized stress $S \equiv \tau/\mu f_B$ ($f_B \equiv \mathcal{F}_B/\mu b w$; $\mathcal{F}_B$: total binding energy, μ: shear modulus, b: Burgers vector, w: trough width) *vs* normalized stress times temperature, for copper alloys: (*a*) Cu-Mn single crystals;[79] (*b*) three polycrystalline Cu alloys;[14] (*c*) Cu-Al single crystals[28,69] and polycrystals;[14,27] (*d*) Cu-Ge (and one Cu-Ga) single crystals.[74,75] ψ is an adjustable constant. Polycrystal flow stresses have been divided by 3.06. All alloys follow a linear decrease in this diagram at intermediate temperatures.

and values of f_B for each concentration, were found that would make all data extrapolate to the same point on the stress-times-temperature axis, and with the same slope. If such values can be found, this is evidence for the possibility of representing the data by this description in this regime.

A general inspection of Figure 12 shows that this is by and large the case. First, Cu-Mn *single crystals* (Figure 22(a))[79] fall on a single straight line for five of the six concentrations; the highest concentration deviates slightly. The values of f_B chosen to give this fit turn out to be proportional to $\sqrt{c}$; this empirical relation will be made use of in the interpretation later on. At 1 at. pct, $f_B = 5 \times 10^{-4}$. The value of $\ln(\dot\gamma_0/\dot\gamma)/\psi$ (using $g(S) = 1 - S$, and $\mu_0 b^3/k = 56560$ K) is 6.3: an eminently reasonable value (Eq. [13c]). While these data referred to a large number of concentrations, studied in a single investigation, they were taken at only three temperatures.

Figure 12(b) presents data on three different copper alloys over a wide range of temperatures[14]—though of only one concentration each, and in this case taken on *polycrystals*. The grain-size dependence was rather strong and solute dependent; the values plotted are from a back-extrapolation of a Hall-Petch diagram to infinite grain size. It is seen that all three alloys exhibit the same initial linear decrease—but widely divergent values of ψ and f_B were necessary to achieve this (Table I). At about room temperature (marked

Table I. Model Parameters from Experimental Analysis of Copper-Alloy Polycrystals and Single Crystals

Alloy	c-Range [At. Pct]	P, S	$f_B/\sqrt{c}$ [Pct]	$\ln(\dot{\gamma}_0/\dot{\gamma})/\psi$	Reference
Cu-Sn	14	P	14	20	14
Cu-Zn	36	P	1.6	15	14
Cu-Mn	1 to 5.5	S	5.0	6.3	79
Cu-Al	0.5 to 15	S, P	2.2	5.5	14, 27, 28, 69
Cu-Ge	1 to 7.3	S	2.6	3.8	74, 75
Cu-Ga	5	S	2.0	3.8	72

by solid symbols), all three alloys show a rather abrupt transition into a plateau. Room temperature is just under $T_m/4$ for Cu, and this is a reasonable homologous temperature for strain-aging effects to set in.

Probably the most intensively investigated alloy is Cu-Al. Figure 12(c) displays some of the data.[14,27,28,69]* It is seen that the polycrystal data from which the grain-size effect had been eliminated[14] fall in quite well with the single crystal data.† The intermediate temperature regime is again well described by a linear decrease; then, again rather abruptly, a real plateau due to dynamic strain aging sets in (at about $T = 300$ K). A single value $\ln(\dot{\gamma}_0/\dot{\gamma})/\psi = 5.5$ was adequate for all data (the best[28] would give a value of 5), and f_B was again proportional to $\sqrt{c}$ (within ±5 pct), being about 2.1×10^{-4} at $c = 1$ at. pct.

Another alloy that has been studied by numerous investigators is Cu-Ge. Two sets of data are shown in Figure 12(d).[74,75†] Dynamic strain aging was investigated in detail[75] and occurred over most of the temperature range, at essentially constant stress (only rising at the highest temperatures). Having gained confidence in the previous three figures, we would describe these data as fitting well enough also; however, the concentration dependence of f_B is here a bit stronger than proportional to $\sqrt{c}$. A single concentration of Cu-Ga[72] is also plotted in this figure and follows the trend.

The concentration dependence within one alloy system cannot, as was pointed out above, be properly studied at a fixed temperature within the framework of this model. Figure 13 shows it for the example of Cu-Al alloys, along with the concentration dependence of the scaling parameter f_B; the former is not simple, and the latter is proportional to $\sqrt{c}$, in this case.

F. *The Cluster Model*

The shortcomings of the discrete-obstacle model have been well realized before.[21,98,104] To account for a more athermal behavior at higher temperatures (without invoking solute mobility or dislocation locking), Labusch[105] has treated the effective interaction between different solute atoms along the same dislocation line, and later[106] the possible action of clusters of solute atoms as strong obstacles (which had been noted[107] and modeled[108] previously). This cluster theory did produce an effective plateau in the τ-T behavior; but it predicts[106] a very strong strain-rate dependence in this regime, which is not observed (at least in macroscopic experiments). Also, the temperature at which the plateau begins should, according to the model, be much higher than observed. A good feature of the model is that the activation energy depends on the cluster size; if this were concentration dependent, so would be the temperature scale (much like in the trough model)—but then the concentration dependence of the flow stress at a fixed temperature, which has been used extensively as an identifying feature of the model, would be uninstructive.

G. *Conclusion*

The observation of a concentration-dependent 'plateau' in the stress-temperature diagram is general in solution hardened alloys. At least in the upper temperature regime of this 'plateau', evidence of dynamic strain aging is frequent: *e.g.*, by jerky flow, or by a high strain-hardening rate that leads to a pronounced 'hump' in the diagram of *ultimate* strength *vs* temperature.

At the *low-temperature* end of the spectrum, the temperature dependence is strong enough that an explanation on the basis of a discrete-obstacle model would seem plausible (if the plateau itself could be explained by an *additive* mechanism). However, the end of the strong decrease and the beginning of plateau-like behavior occur generally at too high a temperature to be consistent with a discrete-obstacle

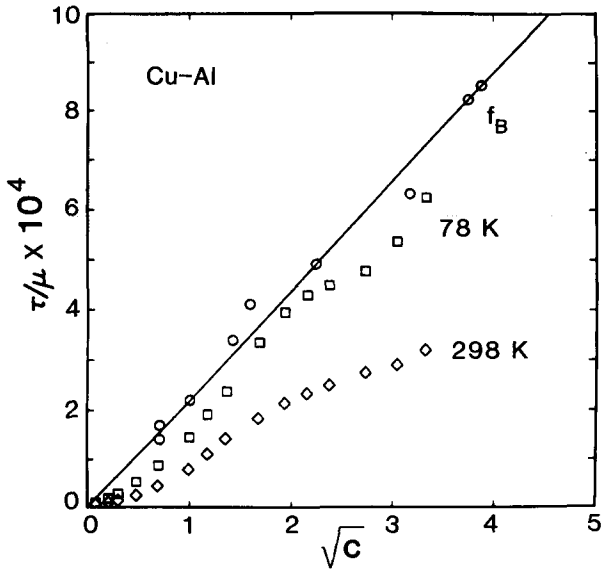

Fig. 13—The concentration dependence of the flow stress (normalized by the shear modulus) at two fixed temperatures, and of the scaling parameter f_B, for Cu-Al.

*Basinski's data below 77 K were omitted from the plot; they exhibit effects from dislocation inertia.[28,102,103]

†A very extensive investigation on many copper alloys[38] shows much higher values of stress, possibly because these were polycrystals of a constant grain size (50 μm), and the grain-size contribution to the flow stress may well have been significant and solute dependent.[14-19]

mechanism: the disagreement is at least a factor of 2 *in the activation energies*. It appears that there must be a regime *below* that of dynamic strain aging in which the behavior is more athermal, *i.e.*, in which the effective resistance to dislocation motion is more long-range than can be expected from discrete solute atoms. We do not find the more sophisticated variations of the discrete-obstacle model, even involving clusters, convincing to solve this problem in a quantitative way.

On a strictly heuristic basis, the temperature dependence of the flow stress in solution hardened alloys at low *and* intermediate temperatures can be rationalized by a dependence of the activation energy on the reciprocal of the stress. (For details, see Section V-D.) Such a dependence is a prominent feature of trough models, in which the dislocation is supposed to unlock repeatedly from stable positions such as they have been envisaged, even in the absence of aging, by Suzuki.[26] An easy test of this empirical fit is a plot of stress *vs* stress-times-temperature; behavior quantitatively consistent with a trough model was demonstrated in a variety of cases.

IV. THE RATE SENSITIVITY OF THE FLOW STRESS

A. *Phenomenology and Discrete-Obstacle Model*

The rate sensitivity of the flow stress in metals at low temperatures is quite small: it is, in fact, hard to measure accurately, and the evaluation of the measurements is subject to debate. However, in a way that is insensitive to these details,[109] the rate sensitivity is a powerful diagnostic tool: its *order of magnitude* and its *variation* with other variables can be analyzed to provide information about the controlling mechanisms.[30,67] The important variables are the obstacle density (varied either by straining or by changing the solute concentration) and the temperature. We will discuss these in the next three sections; but first we summarize the theoretical method, and address the question of order of magnitude.

The basis of the analysis is the assumption that there are no more than two controlling mechanisms, and—to be proved or disproved—that the two flow stresses superpose linearly. Then, differentiation of Eq. [1] and minor manipulation gives

$$\beta \equiv \left.\frac{\partial \tau}{\partial \ln \dot{\gamma}}\right|_T = \left.\frac{\partial \ln \tau_f}{\partial \ln \dot{\gamma}}\right|_T \tau_f + \left.\frac{\partial \ln \tau_d}{\partial \ln \dot{\gamma}}\right|_T \tau_d \equiv m_f \tau_f + m_d \tau_d \qquad [15]$$

The implication is that the variation in strain rate is done *at constant structure*; but it is the dependence of the result *on structure* that we shall analyze.

If a variation in concentration affected only τ_f, then β would have to be a linear function of the total flow stress τ: its offset in the β-direction would be given by the constant $m_d\tau_d$, its slope by m_f. Similarly, if straining affected only τ_d, β would be linear in the total flow stress, its offset being $m_f\tau_f$, its slope m_d. Certainly in the latter case, such behavior is often observed, and thus worth exploring further: when the strain is the independent variable, the best plot is one of β *vs stress* (at a constant temperature and base strain-rate).[29,67,110]

One of the assumptions that enters into the linearity of the 'Haasen plot' discussed in the last paragraph is that the relative rate sensitivity m is independent of obstacle concentration. This is a necessary consequence of the discrete-obstacle model, as will now be shown.[67] For any one set of obstacles (say, the solutes), the flow stress is a *product* of two terms: one dependent on the obstacle spacing, the other on the obstacle strength. The details depend on the statistics; for weak, dilute solutes, one expects

$$\tau_f = \left(\frac{K}{\mu b^2}\right)^{3/2} \mu \sqrt{c} \qquad [16]$$

Here, we have replaced the *maximum* interaction force $\hat{K}$ in Eq. [8] by an *effective* interaction force K, which depends on strain rate and temperature through thermal activation. Obviously, the *logarithmic* derivative of τ_f with respect to strain rate is independent of concentration whenever such a *product* relation holds. Thus, plots of β *vs* τ should be linear in all such cases.

The actual magnitude of m_f is also important: it gives information on the obstacle *width* (or 'depth').[30] Again, the exact value will depend on the detailed statistics used; but the order of magnitude follows, for any model of the discrete-obstacle type, from differentiating Eq. [16]: defining the effective obstacle width at the given strain rate as $\Delta y \equiv -(\partial \Delta G/\partial K)_T$, the rate sensitivity becomes, with Eqs. [5], [15], and [16],

$$\frac{2}{3} m_f = \left.\frac{\partial \ln K}{\partial \ln \dot{\gamma}}\right|_T = -kT \left.\frac{\partial \ln K}{\partial \Delta G}\right|_T = \frac{kT}{K \Delta y} = \frac{kT}{\mu b^3} \frac{\mu b^2}{K} \frac{b}{\Delta y} \qquad [17]$$

Of the three factors in the last expression, the first is typically, at room temperature, 1/180; the second, for a typical solute (see Section III-C), about 60; thus, $2\Delta y/b$ should be of order $1/m_f$ if the model were to hold. Since typical values of the total rate sensitivity m are always less than 1/30, $\Delta y/b$ would come out to be larger than about 15, which is, of course, ludicrous and incompatible with the idea of discrete obstacles.

This problem has frequently been pointed out and has been circumvented by postulating an additional athermal, yet solute-controlled contribution to the flow stress, the 'plateau'. To explain the plateau itself with a discrete-obstacle model is, then, not possible. This argument is very similar to the one arrived at from a qualitative analysis of the temperature dependence in Section III-C.

B. *Strain Dependence*

The rate sensitivity β for different (pre)strains should, as derived above, be plotted as a function of the flow stress (as it changes with strain) for mechanistic interpretation.[110] This is often done in terms of an (apparent) activation area Δa defined by

$$\beta = kT/(b\,\Delta a) \qquad [18]$$

The inverse normalized activation area, $b^2/\Delta a$, is plotted in Figure 14(a) for Ni and Ni-Co alloys.[67] It is a linear function of flow stress. Note, however, that the slope of these lines decreases with concentration. Yet it should be, by the above

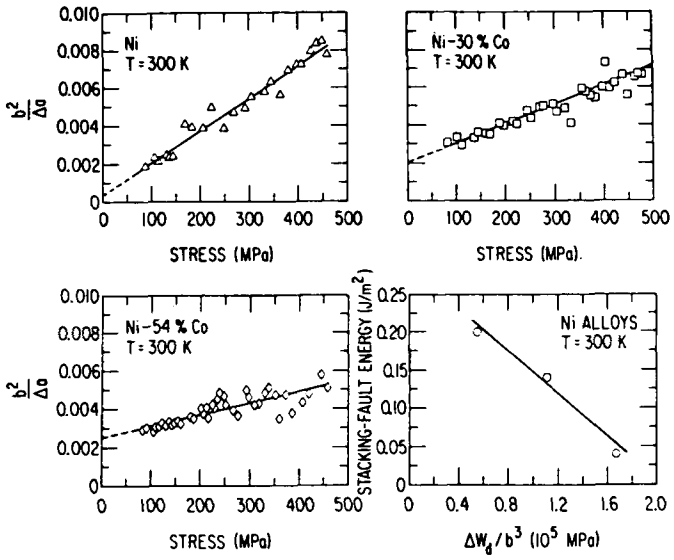

(*a*)

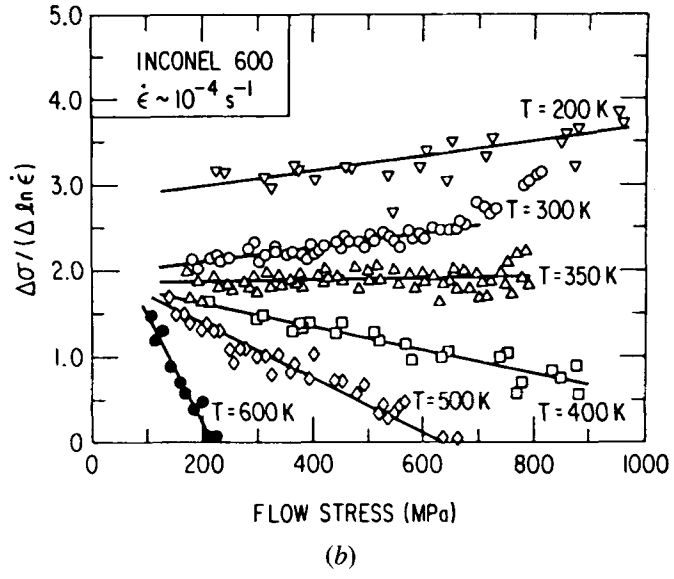

(*b*)

Fig. 14 — Haasen plots for (*a*) Ni-Co alloys and (*b*) INCONEL 600, after Mulford.[67] The slope is a measure of the relative rate sensitivity of the contribution to the flow stress from dislocation/dislocation interactions; it is decreased by solute additions, in a temperature-dependent way. In (b), this effect is due to dynamic strain-aging; in (a) it is commonly rationalized on the basis of the solute dependence of the stacking-fault energy.

analysis, a property of dislocation/dislocation interaction only: m_d. It is evident again that solutes do influence the strain-hardening contribution to the flow stress. For these alloys, an obvious interpretation is that the stacking-fault energy is decreased by the alloy additions, and this increases the effective 'width of the obstacles' (the forest dislocations).

The same behavior is, however, also observed in other alloys such as Ni-C, where the stacking-fault energy is not likely to be affected.[53] On the other hand, dynamic strain aging is here important. This is shown in Figure 14(b) for INCONEL* 600, at various temperatures. The most evident

*INCONEL is a trademark of the INCO family of companies.

characteristic of these data is that the slope m_d is *negative* at some temperatures. This can only be due to dynamic strain aging (even though jerky flow occurs only when the *total* rate sensitivity is negative). Once this is established, it is evidently possible for the same mechanism to lower m_d to some extent, even though not always enough to make the slope negative. This could then be responsible for the effect in Ni-Co also.

In conclusion, there seems to be a general effect of solute additions on the rate sensitivity of τ_d (the strain-hardening contribution to the flow stress), such as to lower it. This is particularly prominent at higher temperatures — and could therefore contribute to more 'athermal' behavior.

C. *Concentration and Solute Dependence*

The same principles that have long been used to study the influence of the forest dislocation density can also be used to investigate the solute atom density: as it is varied, the rate sensitivity β, or the inverse of the activation area Δa, should be a linear function of the flow stress (as it varies with concentration). This can be studied easily at the yield stress, presuming that the dislocation contribution τ_d is here constant or negligible. In the latter case, the straight line should actually go through the origin.

In Figure 15, we have replotted data for silver alloys[28] in this way. The line is well enough straight, and it does approximately go through the origin. Nevertheless, the data disagree with the discrete-obstacle model in two respects. First, the m_f that can be derived from these slopes is about 1/30 at room temperature, 1/45 at 78 K. These values are so *high* only because the data were taken with Basinski's extrapolation method: as 'instantaneously' as possible. The

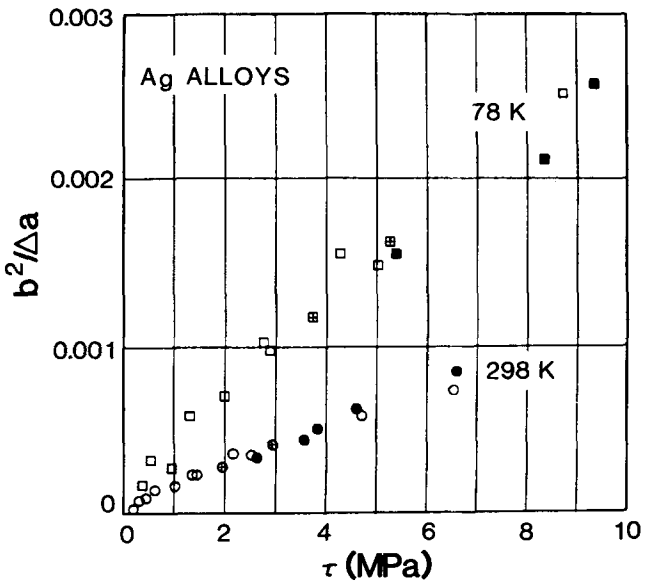

Fig. 15 — Stress equivalence for silver alloys: different alloys show the same dependence of rate sensitivity (the inverse activation area Δa) on concentration when plotted as a function of the (concentration dependent) flow stress. (Open symbols: Ag-In; full symbols: Ag-Sn; cross symbols: Ag-Au.) Also note that the activation area is of order 1000 b^2. After Basinski, Foxall, and Pascual.[28]

values for $\Delta y/b$, by the most favorable statistical interpretation, come out to be 18 and 6, respectively: much too large. If, on the other hand, a reasonable value for $\Delta y/b$ were chosen (such as 1 or 2), the obstacle *spacing* would have to be at least an order of magnitude larger than the spacing of individual solutes along the dislocation line to give the right order of the activation area. This discrepancy has been noted many times, probably first by Schwink and Traub,[107] and was one of the reasons why Basinski *et al.*[28] found it compelling to dismiss the discrete-obstacle model on the basis of their data.

Secondly, Basinski, Foxall, and Pascual[28] discovered that *different alloys* fell on the *same line*. (They plotted it in a different diagram, in which there is no reason for the line to be straight.) They labeled this effect 'stress equivalence': at the same flow stress (and temperature and base strain-rate), any alloy, of whatever solute kind or concentration, has the same rate sensitivity. Yet the same flow stress could come about either by a higher concentration or by a stronger interaction—but only the latter should enter the rate sensitivity (Eq. [17]). Stress equivalence is thus incompatible with a discrete-obstacle model (or at least it would be an incredible coincidence). On the other hand, it would be a natural consequence of a trough model: here, only *one* parameter enters, the decrease in the dislocation line energy per unit length. This will be discussed in detail in Section V-E. Stress equivalence has also been shown to be compatible with Labusch's cluster model.[111]

A third and most powerful argument follows from the data of Basinski, Foxall, and Pascual[28] on *copper* alloys of many concentrations—but this point can be appreciated only by plotting the data in the way used here: Figure 16. In this case, the data curve is far from straight, especially at low concentrations. This means that the obstacle spacing that enters into the activation area is not proportional to the one that enters into the flow stress. We find this the most compelling argument against the discrete-obstacle model, especially since the violation occurs at low concentrations and low temperatures, where the solutes are most likely to act as individual obstacles. Incidentally, even in a discrete-cluster theory[105,106] the spacing of the effective obstacles should be same for the flow-stress relation as for the activation length. Thus, the nonlinearity of Figure 16 would appear to be incompatible with both the discrete-obstacle and the cluster models.

D. *Temperature Dependence*

Finally, at a given structure and base strain-rate, the relative rate sensitivity should depend on temperature in a way that is characteristic of the mechanism(s).[112] The same investigation of Cu-Al alloys[28] also provided such data, and we replotted them in Figure 17 in the way we find most instructive. The qualitative behavior of different models is drawn in as lines. The discrete-obstacle model predicts about same shape as observed, except that it rises sharply at low temperatures, and should be on a much more compressed temperature scale (Section III-C). A two-mechanism model (with one mechanism being 'athermal') demands that m decrease again at higher temperatures. Finally, the trough model predicts a linear initial rise, tending toward eventual saturation. The latter is most closely what is observed; the deviation at high temperatures is in the opposite direction of a separate plateau mechanism. We conclude that, again, a repeated-unlocking model could, on a heuristic basis, explain the plateau-like behavior along with the low-temperature behavior.

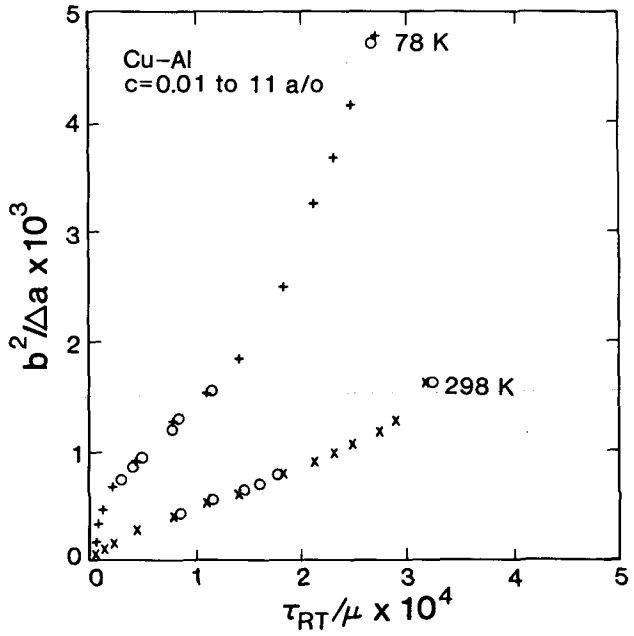

Fig. 16—As Fig. 15, for copper alloys.[28] Also note that the relation is definitely not linear, which it would have to be for discrete-obstacle models.

E. *Conclusion*

Observations of the strain-rate sensitivity of many solution hardened alloys are in conflict with qualitative and basic features of the discrete-obstacle model in four respects: its order of magnitude is too small; it is 'stress equivalent', independent of the *kind* of solute; it sometimes violates the

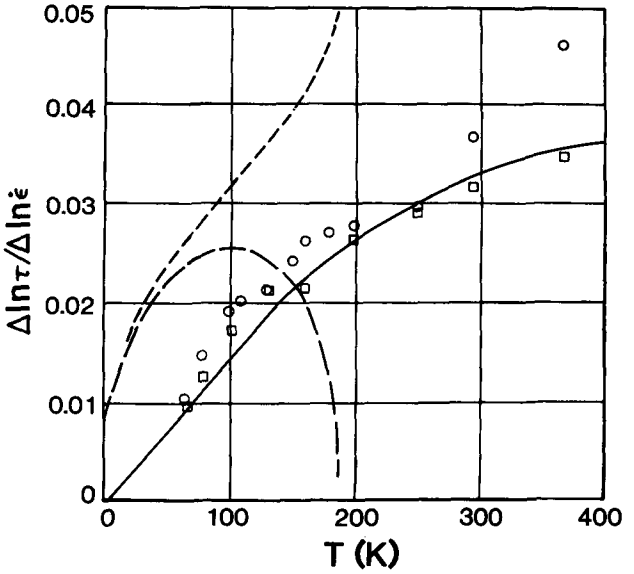

Fig. 17—The relative rate sensitivity of Cu-Al alloys[28] as a function of temperature. The solid line sketches the behavior expected for trough models, the dotted line that for discrete obstacles (single mechanism), and the dashed line for a two-mechanism model (discrete plus athermal).

necessary proportionality between activation length and obstacle spacing; and its temperature dependence is not in accord with either a single short-range mechanism or the superposition of that with an athermal contribution.

We shall discuss some features of the activation area for trough models in the next section.

V. TROUGH MODELS

A. *Requirements for a Viable Model*

We have seen that a bulge-nucleation model (if it could be physically justified) would explain, at least in a qualitative manner, a number of general features of the observations: plateau-like behavior in a flow stress *vs* temperature diagram at intermediate temperatures (actually a $\tau \propto 1/T$ relationship); an unsystematic concentration dependence of the flow stress at constant temperature (since the temperature is also scaled by concentration); 'stress equivalence' of the thermal/rate properties (since there is only one interaction parameter, the binding energy per unit length); and the right type of temperature dependence of the rate sensitivity. We shall now explore whether other features are also compatible with such a model: the temperature dependence at *low* temperatures; the concentration dependence of the scaling parameter; the order of magnitude of the activation area as well as its dependence on concentration (especially at low concentrations); and the interaction with strain hardening.

First, however, let us address the basic problem of justifying such models on physical grounds. The essence of bulge nucleation is that the *length* of the 'bulge' in the dislocation is *not* related to the spacing of individual solute atoms: the bulge is a breaking-away from a *trough*. The solutes must behave as if they were smeared out along the dislocation, and only their interaction energy *per unit length* ($\mathcal{F}_B$) matters, which is proportional to the interaction strength of each solute atom times the concentration of solutes along the dislocation line, C.

The latter is an instructive quantity: in some cases, one may describe it as

$$C = k_1\sqrt{c} + k_2 c = k_1\sqrt{c} \cdot (1 + k_3\sqrt{c}) \qquad [19]$$

Here, c is the bulk atomic concentration, and the k's are constants. The first term in this relation comes from the number of solute atoms the dislocation encounters when moving through a slip plane, while continually flexing between them.[2,30] The term proportional to c could result from the dislocation's collecting, in some way, all solute atoms within a cylindrical volume around it, once it has stopped. (There are also other possibilities for such a linear term.[113]) The observation of a proportionality of the normalized binding energy f_B to the *square-root* of c in Cu-Al (Section III-E) suggests that there is *no* significant collecting after stoppage, at least in this alloy, in this temperature regime.

A trough mechanism would be easy to envisage if the dislocation did collect a significant number of solute atoms from its surroundings after being stopped by forest dislocations: then the distribution could be almost continuous along the dislocation line, and there would be a denuded zone around the dislocation, so that the nucleated bulge would certainly be 'free'. Then, however, there would have to be a significant contribution to the binding energy proportional to c. More fundamentally, it could not happen at the low temperatures where it is observed: diffusion even by one atomic jump, and even if it occurred by something akin to pipe diffusion (but toward the dislocation) does not occur below about $T_m/4$.

It is possible to envisage an essentially *athermal* atomic interchange mechanism, in the very center of the core. However, then the spacing of actual solute atoms along the dislocation, at low bulk concentrations, would be much larger than one atomic spacing: how then can the dislocation behave as if it were *continuously* locked?

One general possibility is that effectively a 'solute dislocation'[114] has been formed: the net effect of all rearrangements in solute distribution, especially at far distances, due to the presence of the particular dislocation under consideration.

A more local solution to this multiple puzzle emerges when one widens the considerations to *extended* dislocations, not only unit ones;[26] and when one allows the solute/dislocation binding to be subject to fluctuations.[27] These possibilities will be treated in detail in the following.

There is one other problem left, and it has been the major cause for the judgment in the literature over the last two decades[3,25] that trough models are inapplicable to normal solution hardening. In this argument, it is envisaged that 'unlocking' of dislocations is primarily a break-away from a stable atmosphere, created typically at a higher temperature. Then, the rest of the volume is denuded of solutes, and the effect is essentially one of the *generation* of mobile dislocations, not of their propagation. Such generation stresses lead to yield drops and Lüders bands, whereas the effects being discussed here hold also for *smooth* yield.

The reason why this objection can no longer be viewed as serious is that dislocation *propagation* itself is known to be *jerky*:[30] dislocations sweep some area of the slip plane easily, only to be stopped at some 'hard line' where they wait for thermal activation. These relatively hard lines would typically be dictated by the arrangement of forest dislocations (or second-phase particles, or even the solutes themselves). An analysis of macroscopic strain rates and pre-exponential factors shows that the waiting time is typically of the order of 1 second. Thus, a viable repeated-unlocking mechanism must allow a dislocation to 'dig a trough' in that sort of time span and, on the other hand, to be comparatively free during the short transit times (when it typically travels one atomic spacing in the order of 10^{-9} s).

B. *Extended Dislocations*

When a dislocation is extended, its partials have, in general, different character: the partial with more edge character will usually interact more strongly with the solute. While a (whole) dislocation is moving, it will encounter solutes on both its partials equally; but when it stops, it may stop so as to maximize the number of solutes on the partial that interacts more strongly. This could happen strictly mechanically; in addition, if there is any quasi-athermal mobility of the solutes within the extended 'core' of the dislocation, some further redistribution might occur as a consequence of stop-

ping. Then, the dislocation is more strongly bound when it is at rest than when it is moving, and the concentration of solutes 'on' it is proportional to $\sqrt{c}$.

In addition, this mechanism provides the rudiments of a *trough*: the partial that has no (or fewer) solutes on it, and the stacking-fault ribbon between them, serve as effective distributors of the interaction force along the dislocation. Figure 18 shows a sketch: it is apparent that the dislocation cannot break away from a single solute independently of the others. (Such configurations have actually been observed by weak-beam transmission electron microscopy in Cu alloys, but the nodes were there interpreted as constricted jogs.[115])

This mechanism relies on the finite *extension* of the dislocations: it can be expected to operate only when this extension is at least of the order of the *range* of the solute/dislocation interaction. (It has nothing to do with the solute *spacing*.[116]) But since the range is typically no more than a couple of atomic spacings, even the dislocation extension in 'high-stacking-fault-energy materials' such as aluminum should be sufficient—especially for edge dislocations, which tend to be more extended.

At the other end of the spectrum of stacking-fault energies (χ), $\chi/\mu b$ may become so *low* as to be negligible with respect to the solute binding-force per unit length, f_B; then, one would again expect a trough model to be tenuous. (In fact, one should then expect dissociation of the partials at a lower stress, with the attendant formation of large faulted areas.) Thus, there is likely to be a subtle interplay between $\chi/\mu b$ and f_B; it would have to be studied in detail to correlate with the observed differences between different alloy systems.

Another possibility for 'trough-digging' is the chemical interaction proposed by Suzuki:[26] since the bulk stacking-fault energy depends on the bulk concentration of solutes, there will also be a local interaction. This is, of course, athermal; but the relaxation time for it would have to be finite, so that there is a difference between moving and temporarily 'waiting' dislocations. Suzuki and his co-workers have elaborated this model in great detail.[27,97] It requires a correlation between the effectiveness of a solute to lower the SFE and to raise the strength. Such a correlation does not seem to exist in all cases.[117]

Note that the essence of all trough models is that the free energy of the resting dislocation is *lowered* by solute interactions: we have assumed that this is generally true when the resting dislocation contains *more* solutes than the bulk—but it may just as well be the other way around: if the interaction were repulsive, or if the stacking-fault energy were *raised* by solutes.

C. *Fluctuations*

A trough model may still be a good approximation when the 'depth' of the trough is not exactly constant. Suzuki[27] has examined the consequences of spatial fluctuations in the binding energy. Not surprisingly, the effect manifests itself in the pre-exponential factor (the activation entropy)—and makes it temperature dependent. At low temperatures (typically about 200 K or less), the temperature dependence of the pre-exponential factor becomes as important as that of the Boltzmann term, and it then becomes questionable whether they can be operationally separated. This is the regime where the discreteness of the obstacles may make itself felt. *Above* this temperature, however, the trough model remains intact despite the fluctuations: that, from our point of view, is the significant result.

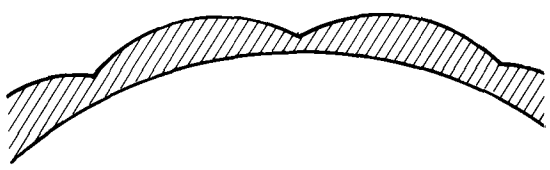

Fig. 18—Interaction of solutes with an extended dislocation: it is generally stronger on one of the partials; the other serves to distribute the force, which could lead to trough-like behavior.

D. *The Trough Profile*

If we now view the interaction between solutes and a resting dislocation as *constant* along its length, one may describe the dependence of the interaction on the forward displacement of the (entire) dislocation (at fixed solute distribution) by a 'trough profile', such as that shown in Figure 19(a). If the 'bound state' is taken as reference, the increase in free energy per unit length, $\Delta\mathcal{F}$, depends on the forward displacement, y, away from the bound state, and reaches the full 'binding energy', $\mathcal{F}_B$, at infinity; then, the

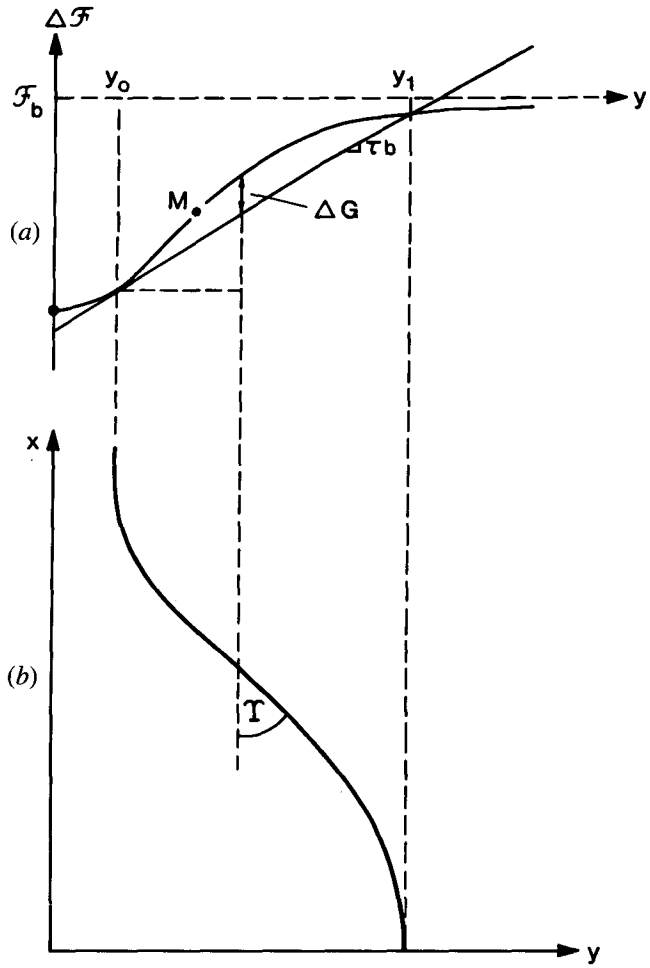

Fig. 19—(*a*) A typical trough profile, schematic: $\Delta\mathcal{F}$ is the interaction energy as a function of the forward displacement of a straight dislocation element, $\Delta\mathcal{G}$ controls the local angle Υ of an equilibrium bulge (*b*) that might be nucleated under a stress τ.

total free energy per unit length is $\mathcal{F}_D$, the line energy of the dislocation.

At a given applied stress τ, the dislocation will move forward to an equilibrium position y_0 given by

$$\left.\frac{\partial \Delta\mathcal{F}}{\partial y}\right|_{y_0} = \tau b \qquad [20]$$

The *maximum* stress needed to unlock the whole dislocation from the trough (the 'mechanical threshold'[30] $\hat{\tau}$) is given by the maximum slope in the $\Delta\mathcal{F}$ *vs* y diagram (point M in Figure 19(a)).

With the aid of thermal activation, a 'bulge' may be nucleated on this dislocation; one-half of it is illustrated in Figure 19(b). One must know its (saddlepoint) equilibrium shape in order to derive the activation energy ΔG. Both the bulge shape (at given trough profile) and ΔG were derived in detail in Kocks *et al.*[30] (Eqs. [24e] through [24f] and [51f] through [51i]). It turns out that the activation energy is given by

$$\Delta G = 2\mathcal{F}_D \int_{y_0}^{y_1} \Upsilon(y)\, dy \qquad [21]$$

where Υ is the angle of the bulge element at position y with respect to the main dislocation direction (Υ being assumed small, called β in Reference 30). The upper limit of the integral is given by the criterion that Υ vanishes again (as it does at y_0).

Thus, the bulge shape is best specified as the function $\Upsilon(y)$. This is again uncomplicated when Υ is small; the result is

$$\Upsilon = \sqrt{2\,\Delta\mathcal{G}/\mathcal{F}_D} \qquad [22]$$

where

$$\Delta\mathcal{G} \equiv \Delta\mathcal{F}(y) - \Delta\mathcal{F}(y_0) - \tau b(y - y_0) \qquad [23]$$

which is shown, at one arbitrary value of y, in Figure 19(a). Putting these equations together, and using the formerly-defined abbreviations f_B and ψ (Eqs. [13a, c]), we get

$$\Delta G = \psi \mu b^3 \sqrt{f_B} \cdot \frac{3}{2} \int_{Y_0}^{Y_1} \sqrt{\Delta\mathcal{G}/\mathcal{F}_B}\, dY \qquad [24]$$

Here, $Y \equiv y/w$, where the trough-width parameter w may be chosen arbitrarily (but the same as in ψ); we will specify a useful one below Eq. [27]. The quantity after the dot comes out to be $g(S)/S$ (Eq. [14]). In other words,

$$g(S) = \frac{3}{2} S \cdot \int \sqrt{\frac{\Delta\mathcal{F}}{\mathcal{F}_B} - SY}\, dY \qquad [25]$$

We will now treat the two limits: low temperature and 'high' temperature. For the limit of *low temperatures*, one may approximate the neighborhood of point M in Figure 19(a) as a cubic and find that

$$\Delta G \propto (1 - \tau/\hat{\tau})^{5/4} \qquad [26]$$

in other words: almost straight.

The situation for the limit of 'high' temperatures (which we shall find appropriate for the *intermediate temperature regime* where plateau-like behavior is observed) is illustrated in Figure 20(a): the stable equilibrium position of the (straight) dislocation is bound to be in a parabolic well; and the farthest excursion of the bulge will have essentially the free-dislocation energy — and these qualitative facts do not change as the stress gets even lower than the value shown in the illustration (which is actually not so low at all!).

The profile shown as a solid line in Figure 20(a) has two advantages: it should describe the intermediate-temperature limit well; and it must give an *upper limit* for ΔG, since the top will certainly be somewhat rounded, such as shown in the dashed curve. This upper-limit property holds provided the model profile and the real one are compared at the same behavior in the bottom of the well. For this reason, it is particularly appropriate to define w in terms of this curvature at the bottom of the energy well. We set

$$\Delta\mathcal{F} = \mathcal{F}_B (y/w)^2, \qquad (y \le w);$$
$$\Delta\mathcal{F} = \mathcal{F}_B, \qquad (y \ge w) \qquad [27]$$

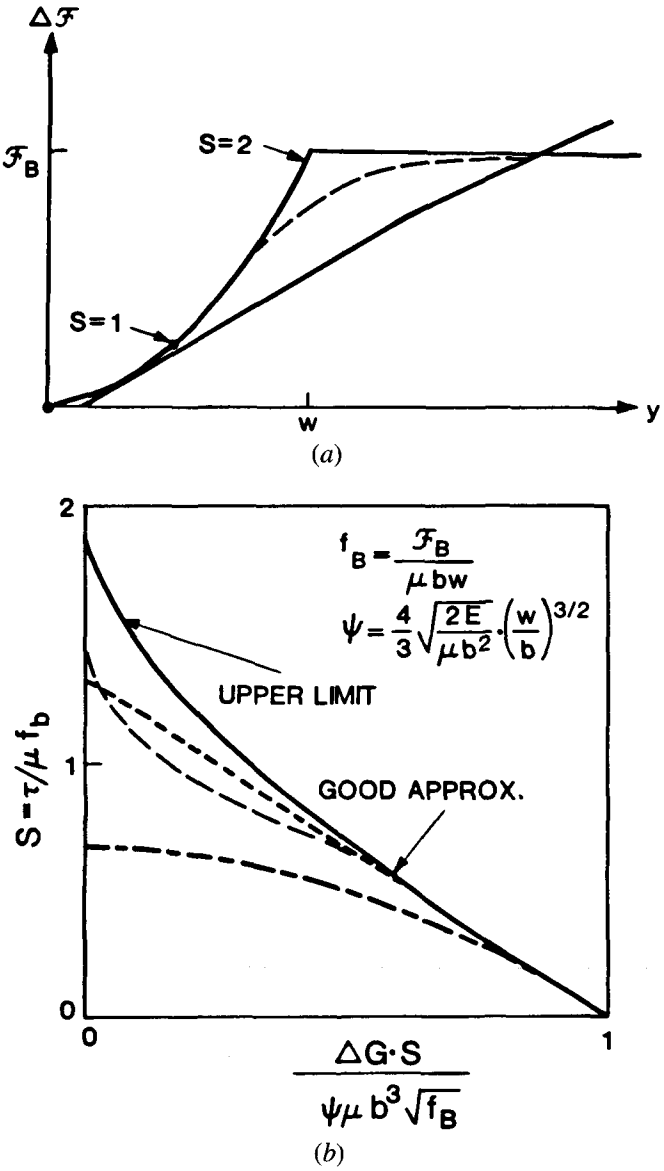

Fig. 20 — Limit for intermediate and high temperatures: a parabolic energy well (*a*). For a given curvature, this gives an upper limit for the activation energy ΔG as a function of the normalized stress S (*b*). The dashed line may describe realistic behavior; the dotted line is the linear approximation we used in experimental analysis; the dash-dotted line is the square-root relation.[26]

These two regimes must be separately integrated, with the help of Eqs. [20], [23], and [24].

A subtle question is how to normalize the stresses. If we stay with the parameter S defined in Eq. [13b], then the maximum stress in the parabolic model profile (Eq. [27], Figure 20(a)) is $S = 2$, not $S = 1$. On the other hand, the region near the true maximum stress is not well described by this model profile anyway; thus, a normalization of the stress by the *maximum* stress would not really be appropriate in the low-stress limit. The normalized parameter S, which is in terms of the total binding energy (and the well-width w), is in fact quite appropriate.

With this convention, integration of Eq. [24] with Eq. [27] gives

$$\Delta G = \psi\mu b^3\sqrt{f_B}\cdot\frac{1-\frac{3}{4}S+\frac{1}{16}S^3}{S} \qquad [28]$$

This function is plotted in Figure 20(b) (as $\Delta G \cdot S$ *vs* S: solid curve). Note that in the limit of low stresses, the dependence is linear—and such as to extrapolate back to $S = 4/3$. That is not an unreasonable value for a real maximum stress, and so this straight-line relationship may be a good first approximation for the total behavior.

In our experimental evaluations, we used $g(S) = 1 - S$, for simplicity. To interpret this in terms of the current limiting model, we would have to replace S by $3/4 \cdot S$, and ψ by $3/4 \cdot \psi$. This does not change the conclusion from those evaluations: that the value of ψ derived from the experiments is eminently reasonable.

In truth, the maximum stress may lie anywhere (so long as $S < 2$); also, the initial decrease must be with the 5/4 power (Eq. [26]), *i.e.*, with an infinite slope. The dashed line is one possibility. (It is worth noting, and will be elaborated upon in the next section, that the *slope* of the curve is always negative, but the *curvature* may well change sign.)

In the light of these derivations, the function $g(S) = \sqrt{(1-S)}$, which was discussed in Section III-E in connection with a triangular well and the Suzuki model, is only a rough approximation: the profile is not smooth near the maximum stress *nor* at $S \to 0$. While it also gives a straight line for $g(S)$ in the limit $S \to 0$, the slope extrapolates to $S = 2$ (using the half-width of the well for a definition of w, as in Section III-D). In Figure 20(b), this functional relation is shown renormalized such as to have the same high-temperature limiting behavior.

Finally, another simple profile of some limiting qualities has been analyzed, namely, where

$$\Delta\mathcal{F} = \mathcal{F}_B\left(1-\frac{1}{1+y/w}\right) \qquad [29]$$

While it has a cusp at the origin, the corner at the top has been replaced by about the longest-range dependence that could be envisaged. Using $w = \mathcal{F}_B/\tau b$, the result is

$$\Delta G = \mu b^3\psi\sqrt{f_B}\cdot\left(\frac{1+S}{S}E(\sqrt{1-S}) - 2K(\sqrt{1-S})\right) \qquad [30]$$

where E and K are the complete elliptic functions of the 'k'-arguments. This relation is also plotted in Figure 20(b), again renormalized to give the same high-temperature behavior.

E. *The Activation Area, Stress Equivalence*

The ('apparent') activation area Δa (or 'activation volume' $b\Delta a$) characterizes the strain-rate dependence of the flow stress (Eqs. [15] and [18]). In terms of activation parameters, it is defined[30] by

$$b\Delta a \equiv -\left.\frac{\partial\Delta G}{\partial\tau}\right|_T \qquad [31]$$

Since ΔG and τ are proportional to various constants that depend only on the alloy system, and then also proportional to a function of the normalized stress S, it is most convenient to study the *logarithmic* derivative; then, with Eq. [14],

$$b\Delta a = \frac{\Delta G}{\tau}\cdot\frac{d\ln(S/g)}{d\ln S} \qquad [32]$$

It is apparent that there is one term which is just $\Delta G/\tau$; it dominates in the limit $S \ll 1$. Since ΔG is strictly a function of temperature and strain rate (Eq. [5]), the activation area is 'stress equivalent', at least in this limit, *i.e.*, it does not depend on the kind of solute or the concentration except through the one parameter, the flow stress. (In a discrete-obstacle model, the term after the dot in Eq. [32] is merely $-d\ln g/d\ln s$; this is a function of s, which is a function of $\Delta G/F_0$, and thus of the obstacle strength; see Section III-C.)

The order of magnitude of the activation volume in this intermediate-temperature limit of the trough model can be easily estimated. At room temperature (in Cu, *e.g.*), $\Delta G/\mu b^3 \simeq 0.1$, and $\tau/\mu \simeq 10^{-4}$ (for a 1 pct-alloy, approximately); thus, the activation volume is of order 1000 b^3: the surprisingly large order usually observed.

For the linear dependence $g = 1 - S$, the total expression [32] may be written as

$$\frac{b^2}{\Delta a} = \frac{\tau/\mu}{\Delta G/\mu b^3}\cdot(1-S) \qquad [33]$$

This should hold approximately for $S < 1/2$. Thus we see that in the truly low-stress limit, the inverse activation area should be proportional to the stress: the same result as in the discrete-obstacle model, but not observed (Figure 16). However, at finite S, this linearity is actually broken. This is because, in trough models, S is *not* a function of temperature and strain rate only, but also of the obstacle concentration (see Eq. [14]). If we express S in terms of ΔG and τ, avoiding f_B, we find

$$S = \left(\frac{\psi\mu b^3}{kT\ln(\dot\gamma_0/\dot\gamma)}\right)^{2/3}\left(\frac{\tau}{\mu}\right)^{1/3} \qquad [34]$$

Thus, there is a fairly rapid (when S is not too low) departure from the apparent linear relation between $1/\Delta a$ and τ; insertion of numerical values shows that it describes the results of Figure 16 quite well.

This correction is also stress equivalent in that, at a given temperature and strain rate, only τ matters—except that ψ enters, and thus the effective trough width: this could depend on the alloy system, and then the stress equivalence should be lost at lower temperatures. It would be very interesting to know whether this is the case: if not, then even the width of the trough profile would be a 'universal' quantity—possibly dependent on the matrix, but not the solute.

The peculiar relation [33] allows one further interesting observation: dividing by τ, and using Eqs. [5], [15], and [18], we have

$$\left.\frac{\partial \ln \tau}{\partial \ln \dot{\gamma}}\right|_T = \frac{1 - S}{\ln(\dot{\gamma}_0/\dot{\gamma})} \qquad [35]$$

In other words: in the intermediate temperature regime where $S \simeq 1/2$, the relative rate sensitivity is about 1/40: very typical for solution hardened alloys.

F. *The Activation Length and the High-Temperature Limit*

It is easy to show that the macroscopically derived ('apparent') activation area is in fact, for trough models, equal to the microscopic geometrical *area* swept out by the bulge during the activation event. It is now interesting to analyze how this area is made up: how much maximum forward excursion, h, and how much length, l_B?

For this, we must first confirm the self-consistency of the assumption previously stated, that the angle Υ is small. From Eq. [21] and Figure 19(a), it is clear that an upper limit is

$$\Upsilon < \sqrt{(2\mathcal{F}_B/\mathcal{F}_D)} = 2\sqrt{(f_B w/b)} \equiv \hat{\Upsilon} \qquad [36]$$

where the dislocation line energy $\mathcal{F}_D$ has been set equal to $\mu b^2/2$, and the definition [13a] has been used for the normalized obstacle strength, f_B. From our analysis of experiments (Table I), we found $f_B \leq 5 \times 10^{-4}$, approximately; setting $w \lesssim 3b$, we get

$$\hat{\Upsilon} \approx 0.1 \qquad [37]$$

or about 6 deg.

Now approximating the bulge as a circular arc that meets the dislocation in the angle $\hat{\Upsilon}$, we can first write

$$\Delta a = \frac{8}{3} h^2/\hat{\Upsilon} \qquad [38]$$

This is an interesting relation because, for the linear form of $g(S)$, at intermediate temperatures, we can also write (Eqs. [31], [13c])

$$\Delta a = \frac{\psi b^2}{\sqrt{f_B}} \frac{1}{S^2} \simeq \frac{4}{3} \frac{w^2}{\sqrt{f_B w/b}} \cdot \frac{1}{S^2} \qquad [39]$$

Comparing Eqs. [38] and [39], and using Eq. [36], we find that the maximum excursion of the bulge, h, is $1/S$ times the trough width, w.

Another relation for the circular arc is

$$\Delta a = l_B^2 \hat{\Upsilon}/6 \qquad [40]$$

from which follows

$$l_B/w \simeq 4/\hat{\Upsilon} \cdot 1/S \qquad [41]$$

The length of the bulge, l_B, is at least 40 times the width of the well, and can become quite large at high temperatures.

There is a limit to the applicability of this model when l_B becomes of the order of the forest dislocation spacing (Figure 21): then, the bulge is no longer free; in effect, the flow stress is due to forest cutting at a lower line energy. This could explain the proportionality between solution hardening and strain hardening discussed in Section II-B.[12] It would also rationalize the proportionality of strain-aging effects to τ_d[12,53]

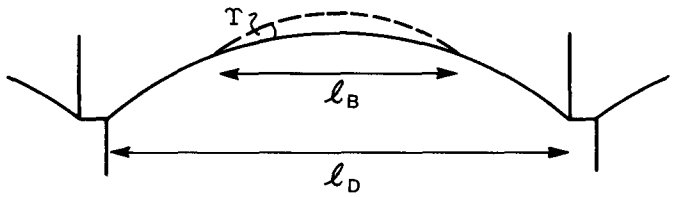

Fig. 21—At low stresses, the bulge length l_B is limited by the forest spacing l_D. This causes an interaction between strain hardening and solution hardening, including strain aging.

G. *Conclusion*

Detailed examples have shown that trough models are quantitatively viable, with respect to both the orders of magnitude and the types of dependencies on temperature, strain rate, and concentration. Their principal advantage lies in the 'intermediate' temperature regime; at very low temperatures, some effects of the discreteness of the solute atoms may be felt (unless inertial effects already dominate); at high temperatures, where the dislocation forest spacing limits the bulge length, a natural transition to solute-dependent *work hardening* is an attractive feature of the model.

VI. SUMMARY

An analysis of a wide variety of data on the temperature and strain-rate dependence of the flow stress in solution hardened alloys has led us to the following conclusions:

1. The *fixed-discrete-obstacle model* is untenable for the following experimental reasons:
   a. A significant glide resistance extends to too high a temperature, by about a factor of 2 at least. There is no cause for any 'plateau'-like behavior.
   b. The observed activation area is at least an order of magnitude too large. (This point has been made by almost every investigator in the field.)
   c. The observed activation area (even that portion of it which can be attributed to solute dislocation interactions) is not proportional to the solute spacing (in one well-investigated case), even at low concentrations and low temperatures. (This point has been made here for the first time, on the basis of Basinski's data.[28])
   d. At a given flow stress, the thermal properties are independent of the concentration and even the *kind* of solute element. (This was discovered by Basinski *et al.*[28] and termed 'stress equivalence'.)

   At least some of these objections hold equally well for the cluster variations of the discrete-obstacle model.
2. It is likely that solute *mobility* contributes to the existence of the 'plateau' at intermediate temperatures in all cases: such mobility is bound to exist above some temperature and, so long as it is not *too* great, is bound to influence dislocation mobility and thus the flow stress. Its presence can be detected most easily by the Portevin-LeChatelier effect and by a hump in the diagram of ultimate tensile strength against temperature; however, it exists beyond these regimes and can there be detected most subtly by any *decrease* in the rate sensitivity with strain.

3. The regime of temperatures *below* that in which thermally-activated solute mobility can be important, may be explained on the basis of a model of 'repeated unlocking' by 'bulge nucleation' from a 'trough'. The jerky nature of dislocation glide through a field of forest dislocations makes this a possible mechanism for an effective propagation stress, not just for dislocation generation. An investigation of the detailed properties of such models appears to satisfy all the requirements of a viable theory. The principal lack, so far, is an attempt to explain the solute dependence, *i.e.*, the influence of size misfit, modulus misfit, electron/atom ratio, *etc.* The model has the additional advantage that it may change but subtly, without any real break, as the temperature is raised and solute mobility becomes an added feature.

It is an unfortunate truism of scientific modeling that a single, basic failure of a model weighs more heavily than 20 years of successes. The repeated-unlocking model has not been subjected to the same scrutiny as the discrete-obstacle model, and thus not been given the same chance to fail. It has been held to steadfastly for 27 years by a single person: Professor Hideji Suzuki. It is time that it be taken seriously.

ACKNOWLEDGMENTS

This work has been generously supported by the Materials Science Branch, Office of Basic Energy Sciences, United States Department of Energy, over the last 12 years, first at Argonne National Laboratory, now at Los Alamos National Laboratory. Many fruitful discussions with R. L. Fleischer, P. Haasen, P. B. Hirsch, R. Labusch, W. C. Leslie, Ch. Schwink, R. B. Schwarz, and D. J. Srolovitz are gratefully acknowledged.

This paper is dedicated to Professor Hideji Suzuki on his sixtieth birthday.

REFERENCES

1. N. F. Mott and F. R. N. Nabarro: Conf. on *Strength of Solids*, Phys. Soc. London, 1947, p. 1.
2. J. Friedel: *Les Dislocations*, Gauthier-Villars, 1956.
3. P. Haasen: in *Physical Metallurgy*, 3rd ed., R. W. Cahn and P. Haasen, eds., North Holland, 1983, p. 1341.
4. R. L. Fleischer: in *The Strength of Metals*, D. Peckner, ed., Reinhold Press, 1962, p. 93.
5. R. L. Fleischer: *Acta Metall.*, 1962, vol. 10, p. 835.
6. W. C. Leslie and R. J. Sober: *Trans. Am. Soc. Metals*, 1967, vol. 60, p. 459.
7. E. R. Parker and R. H. Hazlett: in *Relation of Properties to Microstructure*, Amer. Soc. Metals, 1953, p. 30.
8. T. E. Mitchell: *Prog. Appl. Mater. Res.*, 1964, vol. 6, p. 117.
9. J. D. Embury: in *Strengthening Methods in Crystals*, A. Kelly and R. B. Nicholson, eds., Elsevier, 1971, p. 331.
10. W. C. Leslie: *Metall. Trans.*, 1972, vol. 3, p. 5.
11. M. J. Luton and J. J. Jonas: *Can. Metall. Q.*, 1972, vol. 11, no. 2, p. 79.
12. U. F. Kocks: in *Deformation, Processing, and Structure*, G. Krauss, ed., Am. Soc. Metals, 1983, p. 89.
13. C. G. Schmid and A. K. Miller: *Acta Metall.*, 1982, vol. 30, p. 615.
14. W. Köster and M. O. Speidel: *Z. Metallk.*, 1965, vol. 56, p. 585.
15. V. Ye. Panin, Ye. F. Dudarev, and L. S. Bushnev: *Phys. Metals Metallogr.*, 1966, vol. 21, no. 1, p. 73.
16. M. M. Hutchison and R. T. Pascoe: *J. Austral. Inst. Met.*, 1969, vol. 14, p. 306.
17. K. Nakanishi and H. Suzuki: *Trans. Jap. Inst. Met.*, 1974, vol. 15, p. 435.
18. W. C. Leslie: in *Physics of Solid Solution Strengthening*, E. W. Collings and H. L. Gegel, eds., Plenum, 1975, p. 275.
19. S. G. Khayutin and I. V. Meshchaninov: *Fiz. Metal. Metalloved.*, 1980, vol. 49, p. 158.
20. H. Gleiter: *Acta Metall.*, 1968, vol. 16, p. 857.
21. L. J. Cuddy and W. C. Leslie: *Acta Metall.*, 1972, vol. 20, p. 1157,
22. H. Neuhäuser and H. Flor: *Scripta Metall.*, 1978, vol. 12, p. 443.
23. R. B. Schwarz: in *The Strength of Metals and Alloys*, P. Haasen, V. Gerold, and G. Kostorz, eds., Pergamon, 1979, p. 953.
24. A. van den Beukel: *Scripta Metall.*, 1983, vol. 17, p. 659.
25. P. Haasen: in *Alloying Behavior and Effects in Concentrated Solid Solutions*, T. B. Massalski, ed., Gordon & Breach, 1965, p. 270.
26. H. Suzuki: in *Dislocations and Mechanical Properties of Crystals*, J. C. Fisher *et al.*, eds., Wiley, 1957, p. 361.
27. H. Suzuki: in *Strength of Metals and Alloys*, P. Haasen, V. Gerold, and G. Kostorz, eds., Pergamon, 1980, p. 1595.
28. Z. S. Basinski, R. A. Foxall, and R. Pascual: *Scripta Met.*, 1972, vol. 6, p. 807.
29. U. F. Kocks: in *Strength of Metals and Alloys*, P. Haasen, V. Gerold, and G. Kostorz, eds., Pergamon, 1980, p. 1661.
30. U. F. Kocks, A. S. Argon, and M. F. Ashby: *Prog. Mater. Sci.*, 1975, vol. 19.
31. A. van den Beukel and U. F. Kocks: *Acta Metall.*, 1982, vol. 30, p. 1027.
32. U. F. Kocks: in *Unified Constitutive Equations for Plasticity and Creep of Engineering Alloys*, A. K. Miller, ed., Elsevier, to be published.
33. M. M. Hutchison and R. W. K. Honeycombe: *Metal Sci.*, 1967, vol. 1, p. 70.
34. G. J. den Otter and A. van den Beukel: *phys. stat. sol.*, 1979, vol. (a)55, p. 785.
35. D. T. Peterson and R. L. Skaggs: *Trans. AIME*, 1968, vol. 242, p. 922.
36. T. A. Bloom, U. F. Kocks, and P. Nash: *Acta Metall.*, 1985, vol. 33, p. 265.
37. O. D. Sherby, R. A. Anderson, and J. E. Dorn: *J. Metals*, 1951, vol. 3, p. 643.
38. L. Gastberger, O. Vöhringer, and E. Macherauch: *Z. Metallk.*, 1974, vol. 65, pp. 17, 26.
39. A. J. E. Foreman and M. J. Makin: *Can. J. Phys.*, 1967, vol. 45, p. 511.
40. R. Labusch: Techn. Univ. Clausthal, personal communication.
41. K. L. Hanson and J. W. Morris: *J. Appl. Phys.*, 1975, vol. 46, p. 2378.
42. U. F. Kocks: *Prog. Mater. Sci.*, Chalmers Anniv. Vol., 1981, p. 185.
43. H. Neuhäuser, H. Fiebiger, and N. Himstedt: in *Strength of Metals and Alloys*, P. Haasen, V. Gerold, and G. Kostorz, eds., Pergamon, 1979, p. 1395.
44. J. Diehl: *Z. Metallk.*, 1956, vol. 47, p. 331.
45. R. L. Fleischer: *Acta Metall.*, 1961, vol. 9, p. 184.
46. U. F. Kocks: *Acta Metall.*, 1958, vol. 6, p. 85.
47. H. Mecking and U. F. Kocks: *Acta Metall.*, 1981, vol. 29, p. 1865.
48. P. Haasen and A. King: *Z. Metallk.*, 1960, vol. 51, p. 722.
49. J. Meissner: *Z. Metallk.*, 1959, vol. 50, p. 207.
50. F. Pfaff: *Z. Metallk.*, 1962, vol. 53, pp. 411, 466.
51. C. K. L. Davies, V. Sagar, and R. N. Stevens: *Acta Metall.*, 1973, vol. 21, p. 1343.
52. W. C. Truckner and D. E. Mikkola: *Metall. Trans. A*, 1977, vol. 8A, p. 45.
53. U. F. Kocks, R. E. Cook, and R. A. Mulford: *Acta Metall.*, 1985, vol. 33, p. 623.
54. S. S. Hecker and M. G. Stout: in *Deformation, Processing, and Structure*, G. Krauss, ed., Am. Soc. Metals, 1983, p. 1.
55. U. F. Kocks: *J. Eng. Mater. Techn., (ASME-H)*, 1976, vol. 98, p. 76.
56. Y. Nakada and A. S. Keh: *Metall. Trans.*, 1971, vol. 2, p. 441.
57. P. Jax: *Z. Metallk.*, 1971, vol. 62, p. 279.
58. A. Urakami, M. Meshii, and M. E. Fine: in *Strength of Metals and Alloys*, Am. Soc. Metals, 1970, p. 272.
59. A. A. Hendrickson and M. E. Fine: *Trans. AIME*, 1961, vol. 221, p. 967.

60. G. E. Tardiff and A. A. Hendrickson: *Trans. AIME*, 1964, vol. 230, p. 586.
61. P. Haasen: *Z. Metallk.*, 1964, vol. 55, p. 55.
62. T. Kan and P. Haasen: *Mater. Sci. Eng.*, 1969/70, vol. 5, p. 176.
63. R. H. Hammar, R. A. Strahl, and A. A. Hendrickson: *Trans. Jap. Inst. Met.*, 1967, vol. 9, Suppl. p. 708.
64. P. Jax, P. Kratochvil, and P. Haasen: *Acta Metall.*, 1970, vol. 18, p. 237.
65. J. Dash and M. E. Fine: *Acta Metall.*, 1961, vol. 9, p. 149.
66. H. Asada, R. Horiuchi, H. Yoshinaga, and S. Nakamoto: *J. Inst. Met.*, 1967, vol. 8, p. 159.
67. R. A. Mulford: *Acta Metall.*, 1979, vol. 27, p. 1115.
68. F. Weinberg: *Trans. AIME*, 1968, vol. 242, p. 2111.
69. T. J. Koppenaal and M. E. Fine: *Trans. AIME*, 1962, vol. 224, p. 347.
70. B. J. Brindley, D. J. H. Corderoy, and R. W. K. Honeycombe: *Acta Metall.*, 1962, vol. 10, p. 1043.
71. T. E. Mitchell and P. R. Thornton: *Phil. Mag.*, 1963, vol. 8, p. 1127.
72. E. Peissker: *Acta Metall.*, 1965, vol. 13, p. 419.
73. K. R. Evans and W. F. Flanagan: *Phil. Mag.*, 1968, vol. 17, p. 535.
74. G. Kostorz and P. Haasen: *Z. Metallk.*, 1969, vol. 60, p. 26.
75. H. Traub, H. Neuhäuser, and Ch. Schwink: *Acta Metall.*, 1977, vol. 25, p. 437.
76. G. J. den Otter and R. Vetter: *phys. stat. sol. (a)*, 1978, vol. 50, p. 529.
77. H. Neuhäuser and H. Flor: *Scripta Metall.*, 1979, vol. 13, p. 1147.
78. A. Korbel, L. Blaz, H. Dybiec, J. Gryziecki, and J. Zasadzinski: *Metals Techn.*, 1979, p. 391.
79. Ch. Schwink and Th. Wille: *Scripta Metall.*, 1980, vol. 14, p. 1093.
80. W. F. Sheeley, E. D. Levine, and R. R. Nash: *Trans. AIME*, 1959, vol. 215, p. 693.
81. H. Yoshinaga and R. Horiuchi: *Trans. Jap. Inst. Met.*, 1963, vol. 4, p. 134.
82. H. Scharf, P. Lukác, M. Bocek, and P. Haasen: *Z. Metallk.*, 1968, vol. 59, p. 799.
83. A. A. Akhtar and E. Teghtsoonian: *Phil. Mag.*, 1972, vol. 25, p. 897.
84. J. J. Gilman: *Trans. AIME*, 1956, vol. 206, p. 1326.
85. M. Bocek and G. Hötzsch: *phys. stat. sol.*, 1964, vol. 6, p. 777.
86. T. E. Mitchell and P. L. Raffo: *Can. J. Phys.*, 1967, vol. 45, p. 1047.
87. B. L. Mordike, K. D. Rogausch, and A. A. Braithwaite: *Metal. Sci. J.*, 1970, vol. 4, p. 37.
88. G. Kostorz: *Z. Metallk.*, 1968, vol. 59, p. 941.
89. H. H. Kranzlein, M. S. Burton, and G. V. Smith: *Trans. AIME*, 1963, vol. 233, p. 64.
90. S. K. Lahiri and M. E. Fine: *Metall. Trans.*, 1970, vol. 1, p. 1495.
91. W. A. Spitzig: *Mater. Sci. Eng.*, 1974, vol. 16, p. 169.
92. Y. T. Chen, D. G. Atteridge, and W. W. Gerberich: *Acta Metall.*, 1981, vol. 29, p. 1171.
93. O. Vöhringer: *Metall.*, 1976, vol. 30, p. 1150.
94. R. A. Mulford and U. F. Kocks: *Acta Metall.*, 1979, vol. 27, p. 1125.
95. Y. N. Dastur and W. C. Leslie: *Metall. Trans. A*, 1981, vol. 12A, p. 749.
96. P. Penning: *Acta Metall.*, 1972, vol. 20, p. 1169.
97. H. Suzuki and E. Kuramoto: *Trans. Jap. Inst. Met.*, 1967, vol. 9, Suppl., p. 697.
98. P. Haasen: in *Fundamental Aspects of Structural Alloy Design*, R. I. Jaffee and B. A. Wilcox, eds., Plenum, 1977, p. 3.
99. J. C. Fisher: *Trans. Am. Soc. Metals*, 1955, vol. 47, p. 451.
100. L. J. Teutonico, A. V. Granato, and K. Lücke: *J. Appl. Phys.*, 1964, vol. 35, p. 220.
101. R. J. Gottschall and D. N. Beshers: *J. Appl. Phys.*, 1977, vol. 48, p. 5074.
102. R. B. Schwarz, R. D. Isaac, and A. V. Granato: *Phys. Rev. Let.*, 1977, vol. 38, p. 554.
103. R. B. Schwarz and R. Labusch: *J. Appl. Phys.*, 1978, vol. 49, p. 5147.
104. F. R. N. Nabarro, Z. S. Basinski, and R. Pascual: *Scripta Metall.*, 1978, vol. 12, p. 931.
105. R. Labusch: *Acta Metall.*, 1972, vol. 20, p. 917.
106. R. Labusch, J. Ahearn, G. Grange, and P. Haasen: in *Rate Processes in Plastic Deformation*, J. C. M. Li and A. K. Mukherjee, eds., Am. Soc. Metals, 1975, p. 26.
107. Ch. Schwink and H. Traub: *phys. stat. sol.*, 1968, vol. 30, p. 387.
108. B. R. Riddhagni and R. M. Asimow: *J. Appl. Phys.*, 1968, vol. 39, pp. 4144, 5169.
109. C. Y. Cheng and U. F. Kocks: in *The Strength of Metals and Alloys*, Am. Soc. Metals, 1970, p. 199.
110. P. Haasen: *Phil. Mag.*, 1958, vol. 3, p. 384.
111. F. R. N. Nabarro: *Proc. Roy. Soc.*, 1982, vol. A381, p. 285.
112. R. A. Mulford and U. F. Kocks: *Scripta Metall.*, 1979, vol. 13, p. 729.
113. U. F. Kocks, R. Labusch, and R. B. Schwarz: in *The Strength of Metals and Alloys*, Laboratoire de Physique du Solide, E.N.S.M.I.M.-I.N.P.L., Parc de Saurupt, Nancy, France, 1976, p. 275.
114. R. L. Fleischer: *Acta Metall.*, 1961, vol. 9, p. 1034.
115. C. B. Carter and I. L. F. Ray: *Phil. Mag.*, 1974, vol. 29, p. 1231.
116. P. Haasen: in *Dislocations in Solids*, F. R. N. Nabarro, ed., North Holland, 1979, p. 157.
117. Th. Steffens and Ch. Schwink: *Acta Metall.*, 1983, vol. 31, p. 2013.